Biomaterials 78 (2016) 86–101

Contents lists available at ScienceDirect

Biomaterials

journal homepage: www.elsevier.com/locate/biomaterials

The tissue-engineered human cornea as a model to study expression of matrix metalloproteinases during corneal wound healing

Camille Couture [a, b, c, d], Karine Zaniolo [a, b, c], Patrick Carrier [a, b, c, d], Jennifer Lake [a, b, c], Julien Patenaude [a, b, c, d], Lucie Germain [a, b, c, d], Sylvain L. Guérin [a, b, c, *]

[a] CUO-Recherche, Médecine Régénératrice - Centre de recherche FRQS du CHU de Québec-Université Laval, Québec, Canada
[b] Centre de Recherche en Organogénèse expérimentale de l'Université Laval/LOEX, Québec, QC, Canada
[c] Département d'Ophtalmologie, Faculté de médecine, Université Laval, Québec, QC, Canada
[d] Département de Chirurgie, Faculté de médecine, Université Laval, Québec, QC, Canada

ARTICLE INFO

Article history:
Received 23 September 2015
Received in revised form
4 November 2015
Accepted 5 November 2015
Available online 22 November 2015

Keywords:
Tissue-engineering
Biomaterial
Cornea
Wound healing
Matrix metalloproteinase
Extracellular matrix
Gene expression

ABSTRACT

Corneal injuries remain a major cause of consultation in the ophthalmology clinics worldwide. Repair of corneal wounds is a complex mechanism that involves cell death, migration, proliferation, differentiation, and extracellular matrix (ECM) remodeling. In the present study, we used a tissue-engineered, two-layers (epithelium and stroma) human cornea as a biomaterial to study both the cellular and molecular mechanisms of wound healing. Gene profiling on microarrays revealed important alterations in the pattern of genes expressed by tissue-engineered corneas in response to wound healing. Expression of many MMPs-encoding genes was shown by microarray and qPCR analyses to increase in the migrating epithelium of wounded corneas. Many of these enzymes were converted into their enzymatically active form as wound closure proceeded. In addition, expression of MMPs by human corneal epithelial cells (HCECs) was affected both by the stromal fibroblasts and the collagen-enriched ECM they produce. Most of all, results from mass spectrometry analyses provided evidence that a fully stratified epithelium is required for proper synthesis and organization of the ECM on which the epithelial cells adhere. In conclusion, and because of the many characteristics it shares with the native cornea, this human two layers corneal substitute may prove particularly useful to decipher the mechanistic details of corneal wound healing.

© 2015 Elsevier Ltd. All rights reserved.

1. Introduction

The cornea is localized at the outer surface of the eye. It is a transparent organ, highly specialized and unique that is continually subjected to abrasive forces and occasional mechanical or chemical trauma because of its anatomical localization. Upon injury, a complete reepithelialization and the reorganization of a mature smooth stratified epithelium, as well as a structured stroma, are essential in restoring the adequate function of the cornea [1,2]. Damages to the cornea can result in scarring or opacification that may lead to visual defects and even complete loss of vision in which case corneal transplant is required. More than 10 million patients worldwide are in need of such corneal transplants. Of these, 1.5–2.0 million patients annually have untreated corneal blindness primarily because of the shortage of corneal donors [3]. The need for alternative options to cadaveric corneas is expected to keep growing very rapidly as a result of increasing incidence of transmissible diseases (e.g., human immunodeficiency virus), aging of the population, and the popularity of refractive surgery (primarily photorefractive keratectomy (PRK) and laser *in situ* keratomileusis (LASIK) [4]), which renders corneas unusable for later transplantation. Tissue engineering can remedy this problem by reconstructing a functional human corneal substitute *in vitro* that can be used as a replacement tissue for grafting. Alternatively, the reconstructed cornea is also an outstanding biomaterial to study the cellular and molecular mechanisms of corneal wound healing.

Several models of wound healing have been developed in order to investigate the corneal mechanisms of reepithelialization and to screen for growth factors susceptible to stimulate an adequate healing response [2,5–12]. Although very useful because of their ease of use, cell monolayer *in vitro* models however suffer from the

* Corresponding author. CUO-Recherche/LOEX, Hôpital du Saint-Sacrement, Centre de recherche du CHU de Québec, Québec, QC, Canada.
E-mail address: Sylvain.Guerin@fmed.ulaval.ca (S.L. Guérin).

http://dx.doi.org/10.1016/j.biomaterials.2015.11.006
0142-9612/© 2015 Elsevier Ltd. All rights reserved.

lack of epithelial-mesenchymal interactions and the limited epithelium thickness. In addition, studies of corneal wound healing in animal models are very expensive and inter-individual variability among animals is inherent to *in vivo* experiments. Progress in tissue engineering resulted in the development of human tissue-engineered corneas that were designed to mimic their *in vivo* counterpart in terms of cell phenotype and tissue architecture (see Ref. [13] for an extensive review). The three-dimensional tissue-engineered corneas were intended for basic research or clinical purposes. However, most of them use synthetic biomaterials combined with the use of immortalized human cells, which makes them dissimilar from the native cornea. We recently succeeded in tissue-engineering human corneal substitutes that show appropriate histology, expression of basal membrane (BM) components and integrins [14–20]. Besides being devoided of any synthetic materials, corneas tissue-engineered by our self-assembly approach exhibit a well-developed stratified epithelium, a stroma and a well organized BM [21,22]. When mechanically damaged (using a biopsy punch), this fully human, tissue-engineered cornea, produced from living fibroblasts and untransformed human corneal epithelial cells (HCECs), mimics many aspects of the reepithelialization process including cell migration, proliferation and the restoration of a stratified epithelium [14,15].

Repair of corneal wounds requires proper adhesion as well as migration of HCECs to the BM in order to cover the wound [23] which, in turn, also requires ECM synthesis and assembly. The ECM is a complex, cross-linked structure of proteins and polysaccharides that organizes the geometry of normal tissues. It undergoes complex and dynamic changes in its organization and composition as part of normal homeostasis and tissue repair [24,25]. This process is in great part ensured by the enzymatic actions of metalloproteinases (MMPs), which comprises 23 zinc and calcium ion–dependent proteolytic enzymes that are key regulators of ECM remodeling [26–28]. MMPs are involved in normal and pathologic tissue repair, including epithelial regeneration, fibrotic repair and scar remodeling [29]. MMPs expression is profoundly altered during wound healing in response to the alterations occurring in the secretion of the ECM components such as fibronectin (FN). This is particularly noticeable for MMP9, whose expression increases in corneal epithelial cells during wound healing [30–32] through a process that is likely regulated by cytokines such as IL-1, IL-8 and TGF-β [33–35].

In the present study, we used the two-layers tissue-engineered human cornea as a substitute to investigate the changes that occur in the pattern of genes expressed by corneal cells during wound closure of damaged corneas with a particular attention given to MMPs as they are well known to function as key regulators of ECM remodeling [26–28].

2. Materials and methods

This study was conducted in accordance with our institution's guidelines and the Declaration of Helsinki. The protocols were approved by the hospital and Laval University Committees for the Protection of Human Subjects.

2.1. Cell culture and production of the tissue-engineered human corneas

Human corneal epithelial cells (HCECs) were isolated from the limbal area of normal eyes of 44-, 52- and 71 year-old donors following a procedure previously described [16,36]; the eyes were obtained from the Banque d'Yeux Nationale of the Centre Universitaire d'Ophtalmologie (CHU de Québec, Hôpital du Saint-Sacrement, Québec, QC, Canada). HCECs were primary cultured with a feeder layer of irradiated murine Swiss-3T3 fibroblasts (ATCC, Rockville, MD) as previously reported [16]. Human corneal fibroblasts were isolated from the stromal portion of a cornea (from a 26 days-old donor) left after dispase digestion and removal of both the endothelium and epithelium, and primary cultured and subcultured as previously reported [16,18]. All cells were grown under 8% CO_2 at 37 °C and culture medium was changed after 2–3 days [15].

The tissue-engineered, two-layers 3D human corneas that have been used as a biomaterial were produced following the self-assembly approach [15,20]. Briefly, corneal fibroblasts were seeded and cultured in fibroblast growth medium supplemented with 50 μg/ml ascorbic acid (Sigma, Oakville, Ont., Canada) for 35 days. Ascorbic acid allows fibroblasts to secrete and lay down their own ECM [15]. After peeling from the flasks, two tissue sheets were superimposed to form a reconstructed stroma and were cultured for another week so that they could adhere to each other. Then, human corneal epithelial cells (HCECs) isolated from donors of different ages (44-, 52- and 71-years old) were seeded on the surface of the reconstructed stroma and cultured in submerged conditions in complete epithelial cell medium supplemented with ascorbate, as previously described [14,15,18]. After 7 days, reconstructed tissues were fed an EGF-free epithelial cell medium and were raised at the air-liquid interface for 10 days to induce epithelial differentiation. Reconstructed partial thickness corneas produced by the self-assembly approach were then wounded using 8-mm biopsy punch (Fig. 1A and B). After wounding, the tissue-engineered corneas were placed over two supplementary fibroblast sheets (F3 and F4 on Fig. 1C) to allow reepithelialization over a natural matrix. Wound closure was then examined macroscopically every 24 h for 4 days following the initial damage by observing the ring of reepithelialization that progressed toward the wound center. Biopsy samples were photographed at regular intervals (24 h) using a Zeiss Imager.Z2 microscope (Zeiss Canada Ltd, North York, ON, Canada) equipped with a numeric CCD camera (AxioCam MRm; Zeiss). All experiments were repeated four times. When indicated, corneal stromas were depleted of their corneal fibroblasts by a 3 min treatment with 0.5% sodium deoxycholate followed by five washes with 1x PBS.

When indicated, HCECs were also cultured as a monolayer on tissue culture plates coated with collagen type I (CI; 75 μg/cm^2) and type IV (CIV; 50 μg/cm^2), fibronectin (FN; 5 μg/cm^2), laminin (LM; 2 μg/cm^2), tenascin C (TN; 2 μg/cm^2) or BSA (2%) as previously described [37–39].

2.2. Mass spectrometry

The digest and mass spectrometry experiments were performed by the Proteomics platform of the Eastern Quebec Genomics Center, CHU de Quebec, Canada. Punch biopsies (8 mm diameter) taken either from complete tissue-engineered corneas (stroma/HCEC$^+$) or just the stromal matrix without epithelial cells (stroma/HCEC$^-$) were first dissolved in ammonium bicarbonate 50 mM (10 μl), reduced and alkylated with DTT 45 mM and Iodoacetamide 100 mM, then digested with 126 nM of modified porcine trypsin (Sequencing grade, Promega, Madison, WI) at 58 °C for 1 h. Digestion products were extracted using 1% formic acid, 2% acetonitrile followed by 1% formic acid, 50% acetonitrile. The recovered extracts were pooled, vacuum centrifuge dried, desalted and then resuspended into 10 μl of 0.1% formic acid and 2 μl were analyzed by mass spectrometry. Peptide samples were separated by online reversed-phase (RP) nanoscale capillary liquid chromatography and analyzed by electrospray mass spectrometry (ES MS/MS). The experiments were performed with a Thermo Surveyor MS pump connected to a LTQ linear ion trap mass spectrometer equipped

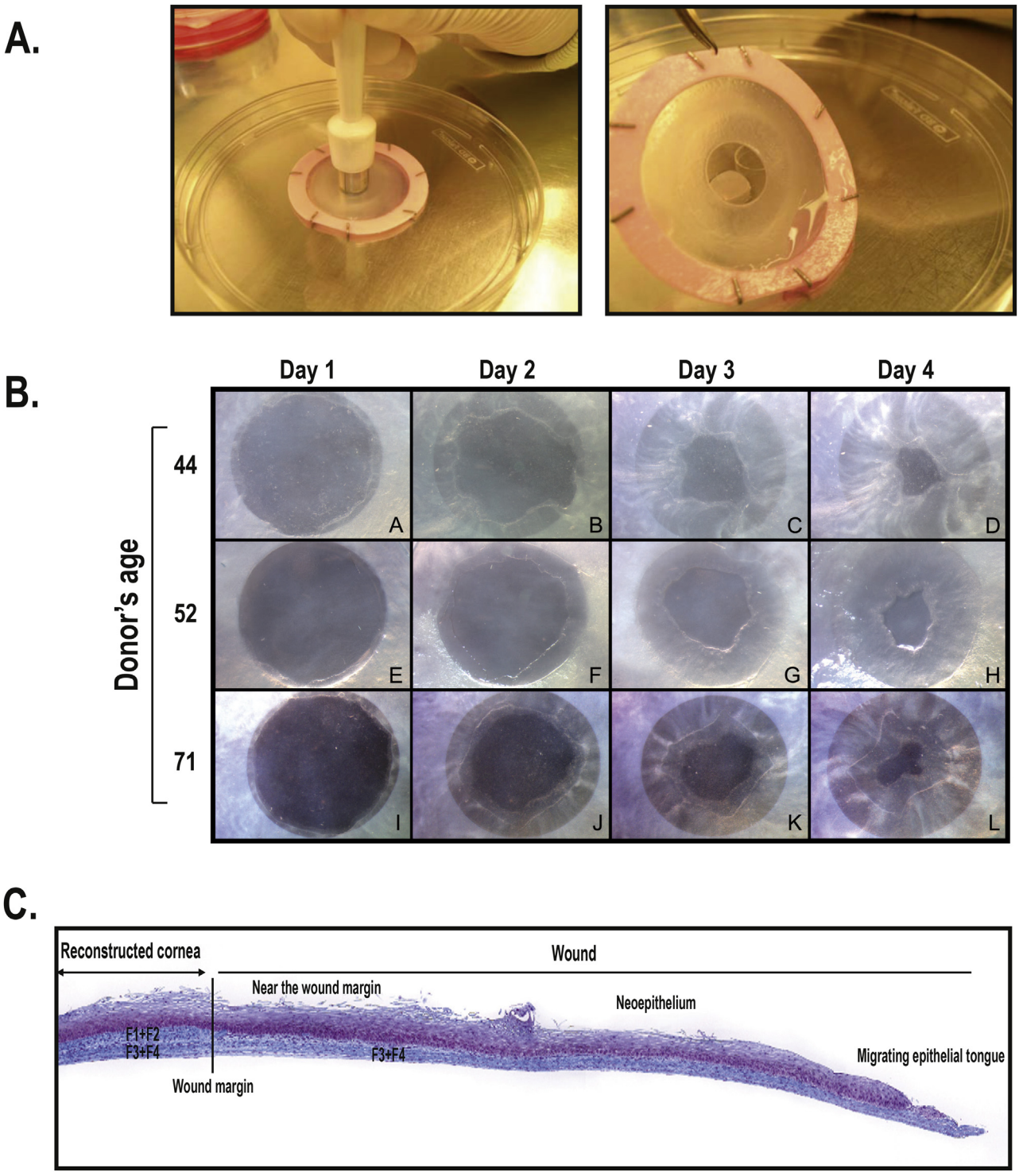

Fig. 1. Production of wounds on tissue-engineered human corneas. **A**: The reconstructed cornea is wounded using a 8 mm biopsy punch. **B**: Closure of wounds on tissue-engineered corneas produced using HCECs isolated from the eyes of three different donors (of 44-, 52- and 71 years old). Closure of the wounded epithelia has been followed from 1 to 4 days after corneal injury. **C**: Composite image showing a complete view of the wounded, tissue engineered human cornea 3 days following corneal damage (sections were stained with Masson's trichrome; cells are pink and collagen is bluish). The wound margin created by the biopsy punch is indicated. F1+F2: initial fibroblast sheets present in the reconstructed cornea prior to wounding; F3+F4: supplementary fibroblast sheets added following wounding of the tissue-engineered corneas. (For interpretation of the references to colour in this figure legend, the reader is referred to the web version of this article.)

with a nanoelectrospray ion source (Thermo Fisher Scoentific Inc., San Jose, Ca USA). Peptide separation took place on a self-packed PicoFrit column (New Objective, Woburn, MA) packed with Jupiter (Phenomenex) 5μ, 300A C18, 10 cm × 0.075 mm internal diameter. Peptides were eluted with a linear gradient from 2 to 50% solvent B (acetonitrile, 0.1% formic acid) in 30 min, at 200 nL/min (obtained by flow-splitting). Mass spectra were acquired using a data dependent acquisition mode with Xcalibur software version

2.0. Each full scan mass spectrum (400–2000 m/z) was followed by collision-induced dissociation of the seven most intense ions. The dynamic exclusion (30 s exclusion duration) function was enabled, and the relative collisional fragmentation energy was set to 35%. All MS/MS samples were analyzed using Mascot (Matrix Science, London, UK; version 2.3.0)). Mascot was searched with a fragment ion mass tolerance of 0.50 Da and a parent ion tolerance of 2.0 Da. Iodoacetamide derivative of cysteine was specified as a fixed modification and oxidation of methionine was specified as a variable modification. Two missed cleavages were allowed. Scaffold (version 4) (Proteome Software Inc., Portland, OR) was used to validate MS/MS based peptide and protein identifications. Peptide identifications were accepted if they could be established at greater than 95% probability as specified by the Peptide Prophet algorithm [40]. Protein probabilities were assigned by the Protein Prophet algorithm [41].

2.3. Western blots

Protein extracts for Western blot analyses were concentrated from culture media using a Centricon Ultracel YM-10 column (EMD Millipore, Darmstadt, Germany). Western blots were conducted as described [38] using the following primary antibodies: a mouse polyclonal antibody against MMP1 (1:5000; Thermo Fisher Scientific Inc., Rockford, IL, USA) or rabbit polyclonal antibodies against MMP2 (1:10000; Thermo Fisher Scientific Inc.), MMP3 (1:3000; Thermo Fisher Scientific Inc.), MMP9 (1:1000; Abcam, Toronto, ON, Canada), MMP10 (1:3000; Thermo Fisher Scientific Inc.), MMP11 (1:5000; Thermo Fisher Scientific Inc.), MMP13 (1:5000; Thermo Fisher Scientific Inc.), Sp1 (1:2000; Santa Cruz Biotechnology, Dallas, Texas, USA), c-Fos (1:2000; Santa Cruz), c-Jun (1:2000; Santa Cruz), JunB (1:2000; Santa Cruz) and actin (1:40000; Santa Cruz) as well as a peroxidase-conjugated AffiniPure Goat secondary antibody against either mouse or rabbit IgG (1:1000 dilution; Jackson ImmunoResearch Laboratories, Baltimore, PA, USA). The labeling was revealed using a Detection Kit (Amersham, Baie d'Urfé, Canada) as described [37,42]. Whenever possible, expression of both the inactive (pro-enzyme) and active MMPs was examined throughout wound closure (which depended on whether antibodies could detect both the active and inactive MMPs or just the inactive one).

2.4. Gene expression profiling

The epithelial cells from biopsy punch-wounded tissue-engineered corneas were isolated from three different areas after 4-days of culture at the air-liquid interface: i) a central area of 8 mm in diameter (wounded) that contains the neoepithelium, ii) the internal (unwounded) ring, that includes tissue surrounding the wounded central area and contained between diameter 8–14 mm of the tissue-engineered cornea, and iii) the external ring, an area that surrounds the unwounded internal ring from diameter 14–19 mm (Fig. 2A). As negative controls, cells were also isolated from the same three areas of unwounded tissue-engineered corneas. Total RNA was then prepared from the material isolated from the central, internal or external rings using the RNeasy Mini Kit (QIAGEN, Toronto, ON, CA). It is important to point out that because corneal fibroblasts are less abundant (36.2 ± 1.0%) than epithelial cells (63.9 ± 0.9%) are in the reconstructed tissue, and that they are trapped in the stromal collagen matrix and not mitotically active, they will not significantly contribute to the total RNAs isolated as nearly all of it will originate from the epithelial cells. RNAs were also isolated from HCECs grown to 100% confluence on 2% BSA, on individual ECM components (collagens type I (CI) and IV (CIV), FN, tenascin (TN) and laminin (LM)) or on tissue-reconstructed stromas depleted (by treating them with 0.5% deoxycholate; stroma$^-$) or not (stroma$^+$) of their corneal fibroblasts. Quantity and quality of all preparation of total RNA was assessed using an Agilent Technologies 2100 bioanalyzer and RNA 6000 Nano LabChip kit (Agilent Technologies, Mississauga, ON, Canada). Biological replicates were as follow: for the wound healing experiment conducted on the tissue-engineered corneas made-up of a stroma with a complete, stratified epithelium, total RNA was obtained from 3 different reconstructed corneas produced using HCECs cultured from 3 different donors (44-, 52- and 71-year old); for the monolayer experiment on BSA, total RNA was obtained from 5 different preparations of HCECs cultured from 3 different donors (44-, 52- and 71-year old); for the stroma$^-$ condition, total RNA was isolated from 3 preparations of HCECs cultured from 3 different donors (44-, 52- and 71-year old); for the stroma$^+$ condition, total RNA was isolated from 2 preparations of HCECs cultured from 2 different donors (44- and 52-year old). For the monolayer experiments on CI, CIV, LM, FN and TN, total RNA was obtained from 5 different preparations of HCECs cultured from 3 different donors (44-, 52- and 71-year old). Cyanine 3-CTP labeled cRNA targets were prepared from 50 ng of total RNA, using the Agilent One-Color Microarray-Based Gene Expression Analysis kit (Agilent Technologies). Then, 600 ng cRNA was incubated on a G4851A SurePrint G3 Human GE 8 × 60 K array slide (60,000 probes, Agilent Technologies). Slides were then hybridized (Agilent protocol), washed and scanned on an Agilent SureScan Scanner according to the manufacturer's instructions. Data were finally analyzed using the ArrayStar V12 (DNASTAR, Madison, WI, USA) software for scatter plots and generation of the heat maps of selected genes of interest. All data generated from the arrays were also analyzed by RMA (*'Robust Multiarray Analysis'*) for background correction of the raw values. They were then transformed in Log2 base and quantile normalized before a linear model was fitted to the normalized data to obtain an expression measure for each probe set on each array. All microarray data presented in this study comply with the *Minimum Information About a Microarray Experiment* (MIAME) requirements. The gene expression data have been deposited in NCBIs Gene Expression Omnibus (GEO, http://www.ncbi.nlm.nih.gov/geo/) and are accessible through GEO Series accession number (GSE #75336).

2.5. Gelatin zymography

The zymographic analyses were conducted as previously described [43] using samples from the culture media of confluent HCECs that have been grown either on BSA or on various individual ECM components (CI and CIV, FN, TN and LM). MMP2 and MMP9 activity was also monitored in the culture medium of wounded tissue engineered human corneas. Medium samples were harvested at the moment the two-layers corneas were wounded (day 0) and then sequentially at every 24 h until 4 days of wound closure (days 1–4). Reconstructed corneas were changed cultured medium every 24 h (and also 24 h prior to wounding) to prevent enzyme accumulation.

2.6. Quantitative PCR (qPCR)

Some of the total RNAs prepared for microarray analyses were also used for qPCR analyses. Reverse transcription was performed using random hexamer primers following the manufacturer's protocol for synthesis of the first strand cDNA (High Capacity cDNA Reverse Transcription Kit; Applied Biosystem, Foster City, CA, USA). Equal amounts of cDNA were run in quadruplicate and amplified in a 20 μl reaction containing 10 μl of 2X Brillant III Ultra-Fast SYBR Green QPCR Master Mix (Agilent Technologies), 250 nM of

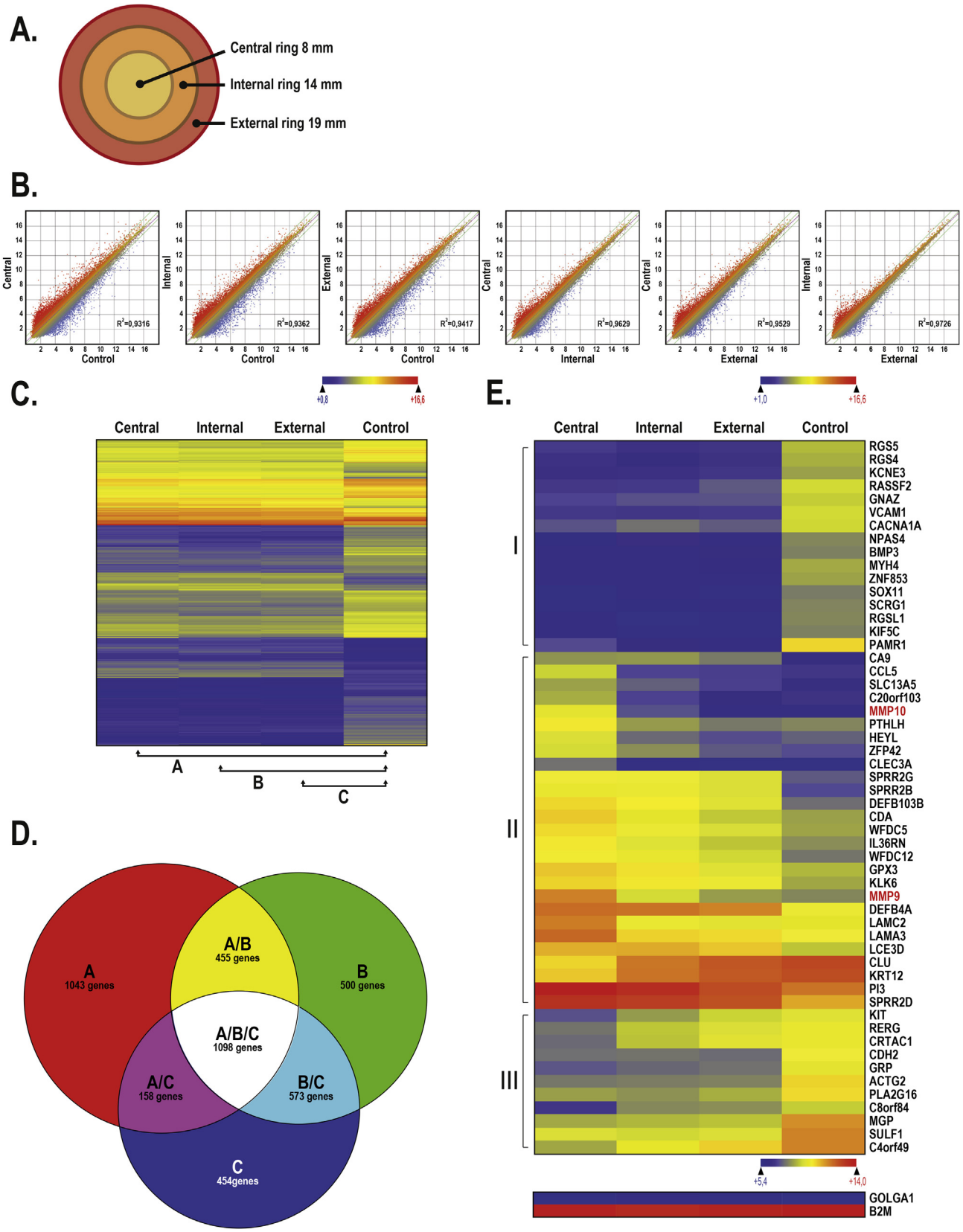

Fig. 2. Microarray analysis of gene expression patterns in response to corneal damage. **A**: Schematic representation of the areas, from the wounded reconstructed corneas, that were recovered five days following wounding in order to prepare total RNA in view of microarray analyses. **B**: Scatter plots of $\log_2$ of signal intensity from 60,000 different targets covering the entire human transcriptome of cells isolated from the central, internal or external area of wounded tissue-engineered human corneas (in the *y-axis*) plotted against: cells from unwounded reconstructed corneas (first three graph), or against cells from the internal or external areas (last three graphs) (in the *x-axis*). **C**: Heatmap representation of genes whose expression is differentially regulated by at least 2-fold in corneal epithelial cells isolated from wounded (central, internal and external) or unwounded (control) tissue-

upstream and downstream primers, and 10 ng of cDNA target. No-template controls were also used as recommended. The mixture was incubated at 95 °C for 3 min, and then cycled at 95 °C for 10 s and at 60 °C for 20 s 35 times using the QIAGEN Rotor-Gene Q real-time cycler. Amplification efficiencies were validated and normalized either to the actin or GAPDH mRNA transcript (as specified in the figure's legends) and quantity of target genes were calculated according to a standard curve. Primers were designed using Primer3 (v.0.4.0) and are listed in Supplementary Table 1.

2.7. Statistical analyses

One-way ANOVA (Figs. 3 and 6) or Student's t-test (Fig. 5) was performed for comparison of the groups in qPCR analyses (Prism 6.0; GraphPad Software, La Jolla, CA). Differences were considered to be statistically significant at $P < 0.05$. All data are also expressed as mean ± SD.

3. Results

3.1. Analysis of corneal wound healing in tissue-engineered human corneas

We first evaluated the feasibility of using tissue-engineered human corneas as a model for studying the molecular mechanisms of partial thickness wound healing of the anterior cornea in an environment close to the *in vivo* condition. As shown on Fig. 1B, macroscopic observation of wound closure in tissue-engineered, two-layers human corneas wounded using a punch biopsy revealed that migration of the corneal epithelium was unequal in each of the three independent wounded corneas. Indeed, multiple convex leading fronts from different regions of the surrounding intact epithelium advanced toward the center (Fig. 1B). These migrating fronts developed within 12–24 h after wounding and continued to advance for the period studied (96 h). Only between 6 and 10% of the wounded areas was remaining at 4 days (Fig. 1B, subpanels D, H and L) and all wounds were completely closed at 5 days (results not presented). The neoepithelium was clearly visible 3 days after wounding (Fig. 1C). Furthermore, the epithelium was stratified and similar to the normal corneal structure near the wound margin and in the middle of the neoepithelium. Therefore, the well-differentiated epithelium from the tissue-engineered corneas produced using the self-assembly approach appropriately responded to injury and demonstrated the validity of using this substitute as a model to study further the mechanisms of wound healing.

3.2. The gene expression pattern is altered by wound healing in the tissue-engineered human cornea

We next wounded tissue-engineered human corneas and conducted gene profiling analysis on microarrays using total RNAs isolated from the epithelial cells of three different areas (central, internal and external areas) from our reconstructed tissues after 4-days of culture under air-liquid condition. A scatter plot analysis of the 60 000 different transcripts contained on the arrays indicated clearly that HCECs from the central area of wounded corneas have patterns of expressed genes distinctive from those yielded by HCECs from unwounded corneas as revealed by the dispersion of the normalized signals that appear as a cloud of dots on Fig. 2B (left panel) and the slope of the regression curve ($R^2 = 0{,}9316$). However, as we move away from the wounded central area toward both the internal and external rings, the number of deregulated genes progressively decreases, as is also revealed by the change in the slope of the regression curve ($R^2 = 0.9362$ and 0.9417, respectively). Comparison of internal and external transcriptional profiles revealed a more modest global change in the patterns of genes expressed by these cells ($R^2 = 0.9726$; Fig. 2B, right panel).

A heatmap for all the genes showing a 2-fold or more expression variation unique to HCECs from the central, internal and external areas of wounded corneas paired with their corresponding regions in the unwounded cornea was then generated (Fig. 2C). A total of 2754 genes fitted into that category of differentially regulated genes when HCECs from the central area are compared between wounded and unwounded corneas (condition A in Fig. 2C and D). The number of total genes deregulated by more than 2-fold decreased to 2626 and 2283 when the microarray data from the internal and external areas, respectively, are compared between the wounded and unwounded tissue-engineered corneas (conditions B and C, respectively, in Fig. 2C and D).

We next examined the data files from the microarrays to sort out genes whose expression is the most deregulated in HCECs from the central, internal and external areas of the wounded corneas relative to their unwounded substitutes. The 55 most deregulated genes were ordered according to their variation during wound healing and arbitrarily named class I, II and III. As shown on Fig. 2E, expression of the genes identified as class I was dramatically reduced in the central wound and remained low as we move away from the wounded area in both the internal and external rings. On the other hand, genes from class II seek their expression strongly increased in the central wound but tend to return to the level of the unwounded control as we move away from the central area. Genes from class III are heavily down-regulated in the central wound and also tend to return to their normal level in the unwounded control as we move away from the central area.

3.3. Epithelial cells respond to corneal damage by altering the expression of MMPs

As both metalloproteinases MMP9 and MMP10 were among the 55 genes identified as the most deregulated in the central area of wounded, tissue-engineered corneas (Fig. 2E) we examined whether other MMP genes had their expression altered during wound healing by searching into the microarray data files. As shown on Fig. 3A, five additional MMPs (MMP1, MMP2, MMP3, MMP11 and MMP13), besides MMP9 and MMP10, also had their expression considerably increased in the central area of wounded, reconstructed corneas. Remarkably, expression of all of them rapidly decreases as we move away from the central wound (in both the internal and external rings). As the activity of MMPs is dependent on the TIMPs, we also monitored their expression during wound healing of the tissue-engineered corneas. Of the four TIMPs, only TIMP3 had its expression considerably increased in the central wound (Fig. 3A). With the only exception of MMP11, the

engineered human corneas. The color scale used to display the log2 expression level values is determined by the Hierarchical clustering algorithm of the Euclidian metric distance between genes. Genes indicated in dark blue correspond to those whose expression is very low whereas highly expressed genes are shown in orange/red. Microarray data for the housekeeping genes β2-microglobulin (B2M) and golgin subfamily A member 1 (GOLGA1) that are expressed respectively to very high and low levels in all types of cells are also shown. **D**: Vein diagram that depicts the number of deregulated genes in wounded (central: red circle; internal: green circle; external: dark blue circle) relative to unwounded reconstructed corneas. Genes that are deregulated between two different areas are also indicated (in yellow, purple and light blue) as well as those commonly deregulated in all three areas (in white). **E**: Heatmap representation of the 55 most deregulated genes expressed by wounded (central, internal, external) relative to their levels in unwounded tissue-engineered corneas (control). (For interpretation of the references to colour in this figure legend, the reader is referred to the web version of this article.)

increased MMPs expression observed in microarray were also validated by qPCR (Fig. 3B). Detection of MMP11 in our microarray data files is, however, consistent with previous analysis that observed expression of that gene in corneal epithelial cells [44].

We then examined whether the alterations observed in microarray for the expression of MMPs may have resulted from corresponding changes in the expression of interleukins and TGFβ in the central area of wounded corneas as these diffusible compounds are well documented to influence on MMPs expression through alterations in the expression and/or activity of the transcription factors Sp1 and AP-1. Indeed, dramatic increases in the central area that progressively decrease as we move away from the wounded area could be observed by microarrays for IL-1α, IL-1β, IL-6, IL-11 and both TGF-β1 and TGF-β3 expression (Fig. 3C). Interestingly, expression of the gene encoding Sp1 was lower in the central area than in the periphery of the wounds whereas that of the AP-1 constituting subunit c-Jun was considerably higher in the central wounded area (Fig. 3D). Both these results (decreased Sp1 and increased AP-1 expression) were further confirmed by qPCR (Fig. 3E). The reduced expression of the Sp1 transcript in the central wound also translated into a corresponding reduction of the Sp1 protein relative to the level observed into both the internal and external rings (Fig. 3F). Meanwhile, Western blot analyses revealed that expression of the AP-1 subunits c-Fos, c-Jun and JunB was higher in both the central and internal areas than in the external ring of wounded corneas (Fig. 3F), a result somehow consistent with both the microarray and qPCR data.

As we identified many MMPs whose expression is deregulated during wound healing of two-layers tissue-engineered corneas, we next monitored their secretion into the culture medium by Western blot during wound closure over a four-day period. All of the MMPs whose transcription was demonstrated to be deregulated in the central area of wounded corneas by microarray (MMP1, MMP2, MMP3, MMP9, MMP10, MMP11 and MMP13; Fig. 3) were also expressed at the protein level prior to wounding although both MMP3 and MMP11 were very low (day 0; Fig. 4A). Interestingly, the amount of inactive pro-MMP1 progressively diminished with increasing wound closure time whereas that of active MMP1 increased, as is revealed by the decrease in the pro-/active MMP ratio. Similar results were also observed with MMP11. No significant change was observed in the pro-/active MMP2 ratio, which is consistent with the modest 2-fold increase observed in the MMP2 enzymatic activity (Fig. 4B). Interestingly, the amount of secreted pro-MMP9 progressively diminished as wound closure was progressing suggesting that pro-MMP9 was converted into the active form of the enzyme as wound closure proceeds. This is indeed consistent with the increased enzymatic activity observed in gel zymography for MMP9 in the culture medium of wounded reconstructed cornea (10-fold increase in gelatinolytic activity at day-4 relative to day-0; Fig. 4B). As for MMP9, our antibodies against MMP3 and MMP13 could only recognize the inactive pro-enzyme. Expression of pro-MMP3 increased at 1-day post-wounding but remained constant until 4-day wound closure. Interestingly, basal expression of the MMP1, MMP3, MMP10, MMP11 and MMP13 pro-enzymes increased within 24 h and then progressively decreased (for MMP1, MMP10 and MMP11) as wounds were closing.

3.4. Deregulated expression of MMPs by HCECs depends on the presence of stromal fibroblasts

We next wished to determine which of the fibroblasts or the ECM they secrete contributes the most to the change in the expression of MMPs secreted by HCECs during wound healing. As shown on Fig. 5A, culturing HCECs on the stromal matrix depleted of its fibroblasts (ECM influence alone) resulted in a significant increase in the expression of many MMPs (MMP1, MMP7, MMP9, MMP10, MMP14, MMP15, MMP17 and MMP23B) relative to the pattern seen when HCECs are grown solely on BSA. These results were validated further for both MMP9 and MMP10 (which are also the most deregulated) by qPCR (Fig. 5B) and gel zymography (for both MMP2 and MMP9 Fig. 5C). In addition, TIMP3 gene expression was also substantially increased in HCECs by the devitalized stroma. Remarkably, preserving the stromal fibroblasts within the tissue-engineered stroma (stroma+) dramatically increased expression of MMPs (MMP2, MMP3, MMP12, MMP13 and MMP24) that otherwise did not responded to the tissue-engineered ECM alone (stroma-). On the other hand, expression of MMP1, MMP10 and MMP14 (and also that of TIMP2) was primarily dictated by the interaction of HCECs with the secreted ECM as no further increase was observed when living fibroblasts were maintained in the stroma. Interestingly, expression of the MMP7 gene (as well as that of TIMP3), which was considerably stimulated by the ECM alone, increased further when living fibroblasts were present in the stroma suggesting that its transcription responds to both the ECM and the diffusible factors secreted by fibroblasts.

As the ECM is a complex structure made up of different cell-adhesion components, we next evaluated whether individual ECM components might have accounted for the increased expression of the MMPs (for instance MMP1, MMP7, MMP9, MMP10, MMP14, MMP15, MMP17 and MMP23B) in response to the devitalized ECM. As illustrated on Fig. 6A, MMP1 expression was considerably increased by CI but was strongly repressed by FN and TN. No increased expression was observed for MMP7 whose transcription was, however, repressed by both CIV and FN. Expression of MMP10 was also increased by CI but dramatically repressed by TN. No significant variation in the expression MMP14, MMP15, MMP17 and MMP23B was observed besides a weak decrease on LM for both MMP15 and MMP17. Interestingly, MMP9 expression was substantially increased by both CI and LM but repressed by TN, a result that was also confirmed by qPCR (Fig. 6B). However, these ECM component-dependent influences on the transcriptional activity of the MMP9 gene (activation by CI and LM and repression by TN) did not translate into corresponding alterations in the MMP9 enzymatic activity (Fig. 6C) or in the amount of MMP9 protein (Fig. 6D) despite an increase in the proMMP9/active MMP9 ratio when HCECs are grown on FN and TN (0.80 and 1.06 for FN and TN, respectively, compared to 0.20 on BSA). A substantial increase in the proMMP2/active MMP2 ratio was observed when HCECs are grown on TN (3.68 on TN compared to 1.81 on BSA; Fig. 6D) that also translated into a near 2-fold reduction in the MMP2 enzymatic activity on TN (Fig. 6C). As with TN, LM also increased the proMMP2/active MMP2 ratio (3.58 on TN compared to 1.81 on BSA). In agreement with the results presented on Fig. 5A, MMPs whose expression responded only to the presence of living stromal fibroblasts (MMP2, MMP3, MMP12, MMP13 and MMP24) were also unaffected by any of the individual ECM components on which HCECs were grown.

3.5. The composition of the stromal ECM is under the influence of HCECs

We next exploited mass spectrometry to determine the precise protein composition of the ECM produced by stromal fibroblasts and determined whether the presence of HCECs contributes to the final organization of this matrix. Examination of the tissue-engineered stroma that has not been added HCECs (stroma/HCEC^{-}) revealed that it is rich in collagen types VI and XII with moderate levels of collagen types I and XIV (Fig. 7A). All together, collagens corresponded to 56% of all ECM peptides detected in the tissue-engineered stromas (average collagen peptides counts: 361;

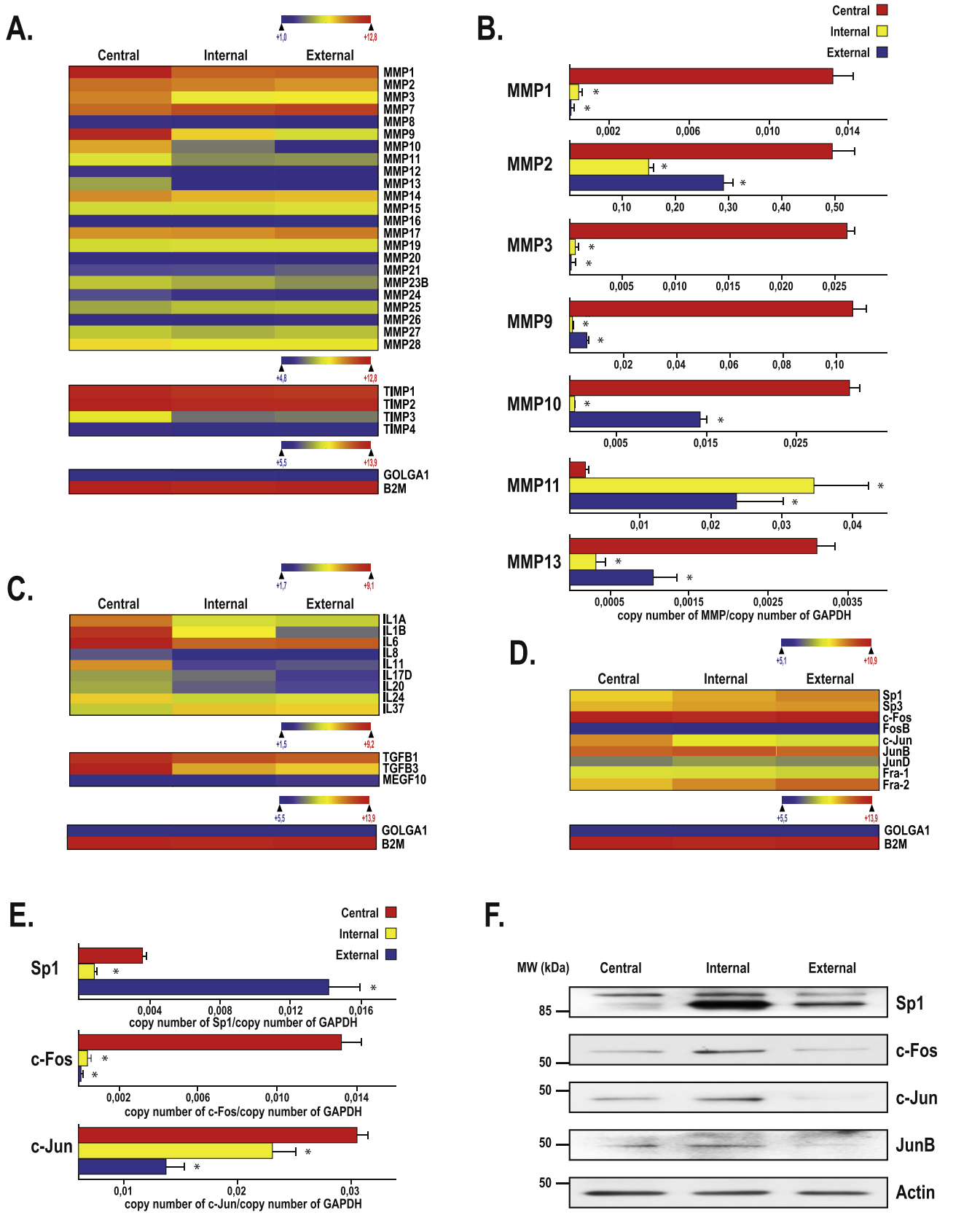

Fig. 3. Analysis of MMPs gene expression in response to corneal damage. **A**: Heatmap representation of the expression profiles of both MMP and TIMP genes between central (wounded), internal and external (unwounded) areas of tissue-engineered human corneas. **B**: qPCR analysis conducted for the MMPs (MMP-1, MMP-2, MMP-3, MMP-9, MMP-10, MMP-11 and MMP-13) that have been identified as the most deregulated between the central and external areas of wounded reconstructed corneas. Data were normalized to GAPDH and their statistical relevance analyzed by one-way ANOVA (Dunnett's post-test; $P < 0.05$). **C**: Same as in panel A but for the genes encoding both interleukins and TGFβ. **D**. Same as in panel A but for genes encoding the transcription factors Sp1, Sp3 and AP1. **E**: qPCR analysis of Sp1 and the AP1 subunits c-Fos and c-Jun. Data were normalized to GAPDH and their statistical relevance analyzed by one-way ANOVA (Dunnett's post-test; $P < 0.05$). **F**: Western blot analysis of Sp1 and the AP1 subunits c-Fos, c-Jun and JunB. Actin is also shown as an internal control.

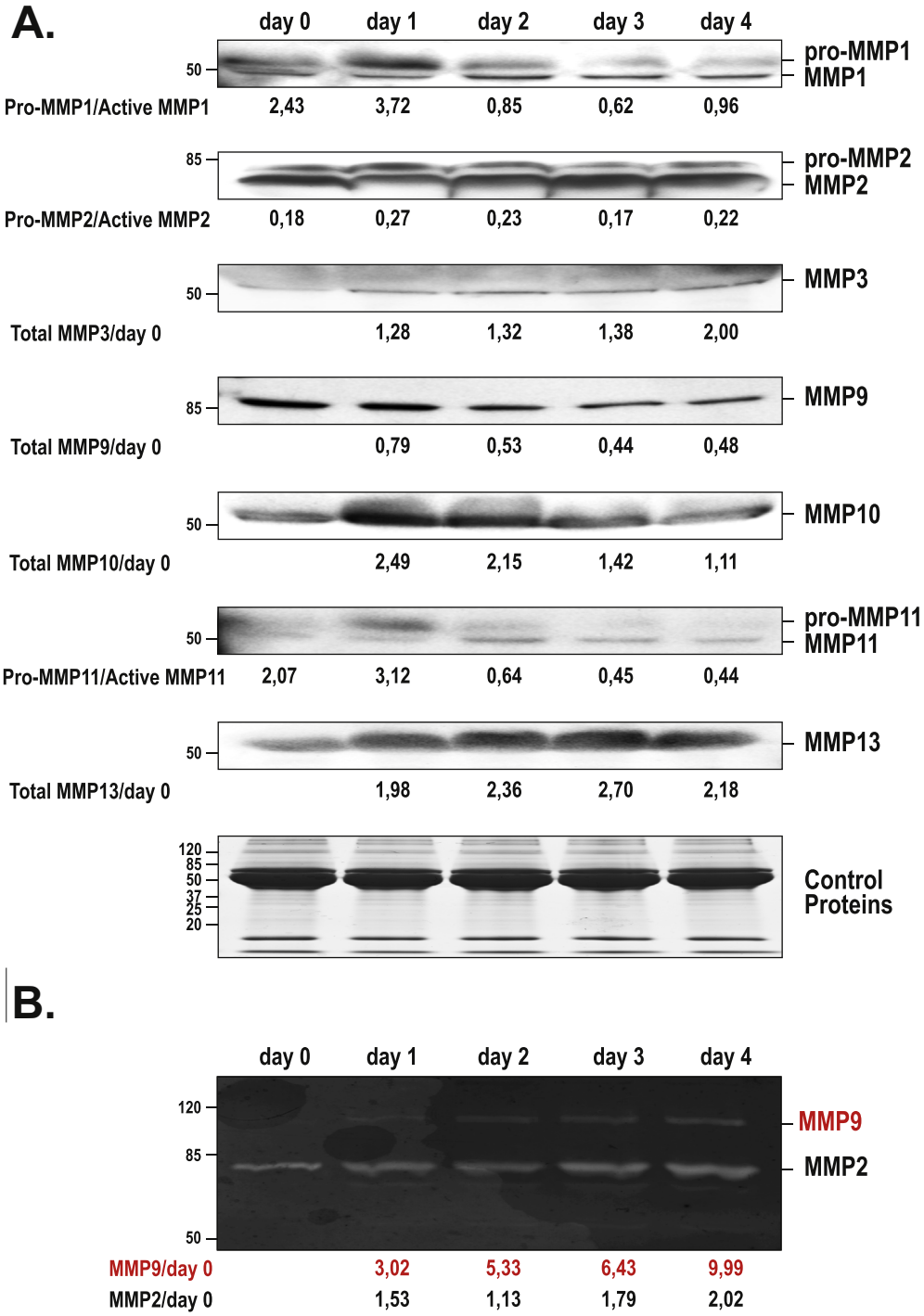

Fig. 4. Expression and enzymatic activity of MMPs during wounds closure. **A**: Samples of culture media from unwounded (day 0) and wounded (day 1–4 of wound closure) tissue-engineered human corneas were analyzed by Western blot to reveal the relative amount of pro- and active MMPs. Data are expressed as the ratio of pro-MMP/active-MMP, with the exception of MMP3, MMP10 and MMP13 that were compared to their level prior to corneal wounding at day 0 (as their respective antibodies only recognized the inactive pro-enzyme). Coomassie blue staining of proteins from each sample is also presented as a normalization control (bottom lane). The most relevant molecular mass markers (kDa) are also indicated on the left of each blot. **B**: The media samples used in panel A were examined by gel zymography to reveal the gelatinolytic activity of both MMP-2 and MMP-9.

average total ECM peptides: 641; Fig. 7A and Table 1). Furthermore, FN, TN (that totalize 16% of the ECM components), periostin, fibulins and fibrillins are the predominant glycoproteins present in the stroma/HCEC^{-} (Fig. 7B and Table 1) whereas low levels of the proteoglycans biglycan, lumican, versican, mimecan, fibromodulin and decorin (that altogether totalized 9% of the average total ECM peptides) could also be detected (Fig. 7C and Table 1). Addition of HCECs had little impact on the stromal accumulation of proteoglycans (11% with stroma/HCEC^{+} compared to 9% with stroma/HCEC^{-} of the average total ECM peptides), besides the detection of low levels of both perlecan and glypican in the stroma/HCEC^{+} condition that otherwise were totally absent from the stroma/HCEC^{-} condition (Fig. 7C). However, the presence of HCECs caused significant changes in the combination of collagens that were

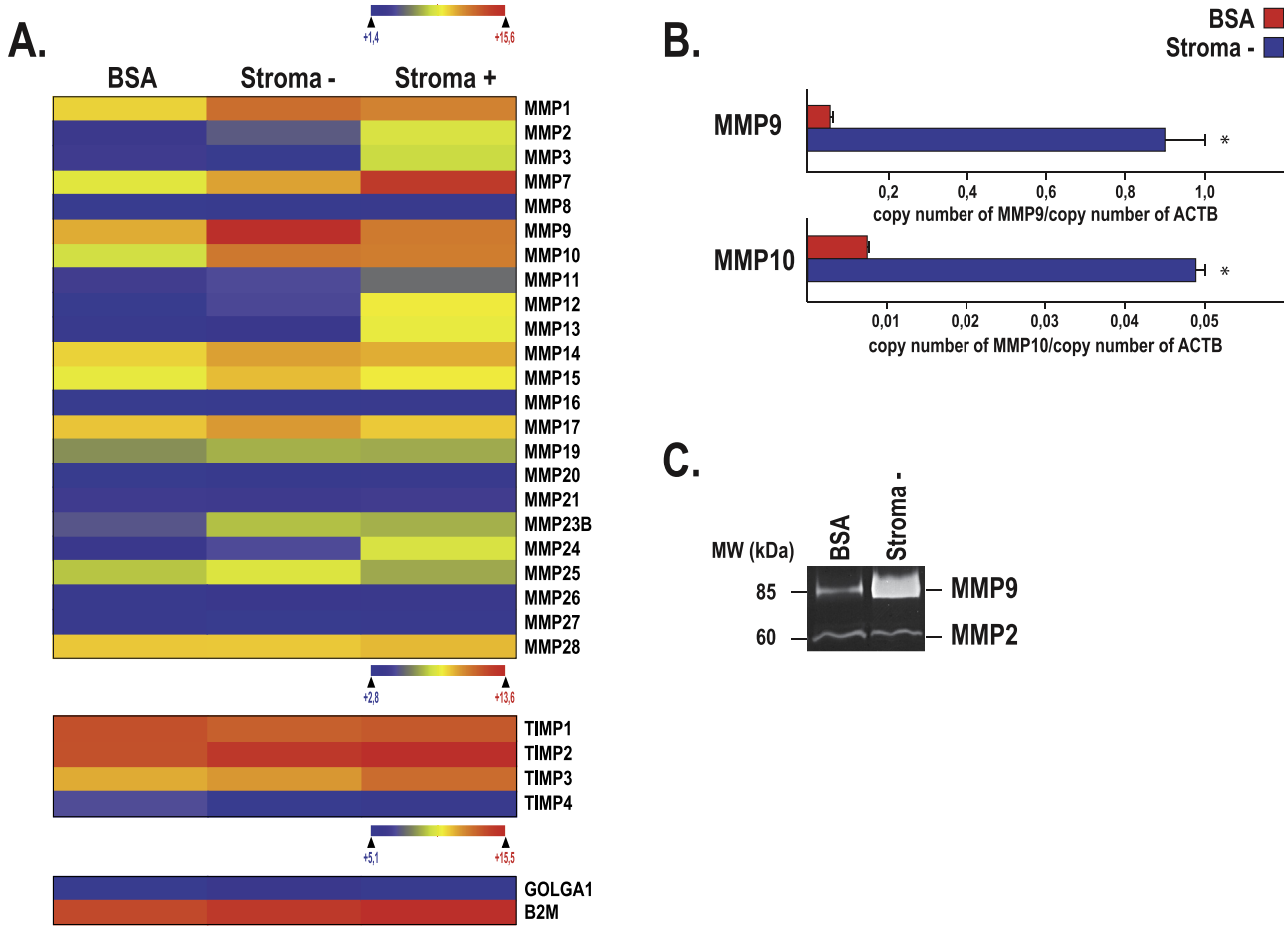

Fig. 5. Expression of MMPs in HCECs grown on a complex stroma. **A**: Heatmap representation of the expression profiles for all MMP and TIMP genes in HCECs grown on BSA (used as a negative control) or on tissue-engineered stromas that have been depleted (stroma-) or not (stroma+) of their fibroblasts. **B**: qPCR analysis of MMP9 and MMP10 expression in HCECs grown on BSA or on a fibroblast-depleted stroma (stroma-). **C**: Samples of culture media from HCECs grown on BSA or on a fibroblast-depleted stroma (stroma-) were examined by gel zymography to reveal the gelatinolytic activity of both MMP-2 and MMP-9. The position of the most relevant molecular mass markers (kDa) is indicated.

secreted into the stromal ECM. Indeed, the amount of collagen types -VI, -XII and XIV was considerably decreased in the stroma/HCEC$^+$ condition whereas that of types II, III, IV, V, VII, XVII and XVIII, most of which could not be detected in stroma/HCEC$^-$, can now be detected at low levels in stroma/HCEC$^+$ (Fig. 7A). However, the overall proportion of collagens remained the same whether or not HCECs are present in the tissue-engineered substitutes (55% with stroma/HCEC$^+$ compared to 56% with stroma/HCEC$^-$ of the average total ECM peptides; Table 1). Appearance of laminins, increased levels of TN and the complete disappearance of fibrillin, along with a substantial reduction in FN, periostin and fibulins are the most noticeable features occurring in the glycoproteins composition of the stroma/HCEC$^+$. Again, despite the change in the composition of the glycoproteins when HCECs are present, their overall proportion remained the same between both conditions (34% of the average total ECM peptides for both the stroma/HCEC$^+$ and stroma/HCEC$^-$ conditions; Table 1).

4. Discussion

Wound healing is a well-ordered but complex process involving activities such as cell migration and proliferation. Migration of corneal epithelial cells requires the coordinated expression of growth factors and cytokines [45–49]. During cell migration, the epithelial cells (and to some extent, the stromal fibroblasts as well) in turn regulate the expression of both extracellular matrix (ECM) proteins and matrix metalloproteinases (MMPs) that are required to ensure appropriate remodeling of the ECM during the wound healing process [47,49,50]. The very fast but transitory changes occurring in the composition of the ECM on which corneal epithelial cells migrate in order to cover the damaged corneal area are probably the most important characteristic of corneal wound healing. These rapid modifications in the ECM composition are in part ensured by the enzymatic activities of MMPs whose expression and activity change as wound healing is progressing. We previously demonstrated that tissue-engineered, complex ECMs could be used as biomaterials in order to study the expression of integrin genes as well as other genes that might play a pivotal function during the corneal repair process [51]. In the present study, we used the two layer tissue-engineered human cornea, a substitute that is much closer to the native cornea as it is constituted of a stroma and a stratified epithelium made up of 5–7 layers of epithelial cells, as a model system to study the contribution of MMPs to the healing of partial thickness wounds of the anterior cornea. We did not include an endothelial layer in our reconstructed cornea since the endothelium is part of the posterior cornea. It could be interesting in the future to evaluate the effect of the endothelium on wound healing since dramatic changes in the organization and quality of the corneal BM have been reported when immortalized mouse corneal endothelial cells are present in the three-dimensional corneal

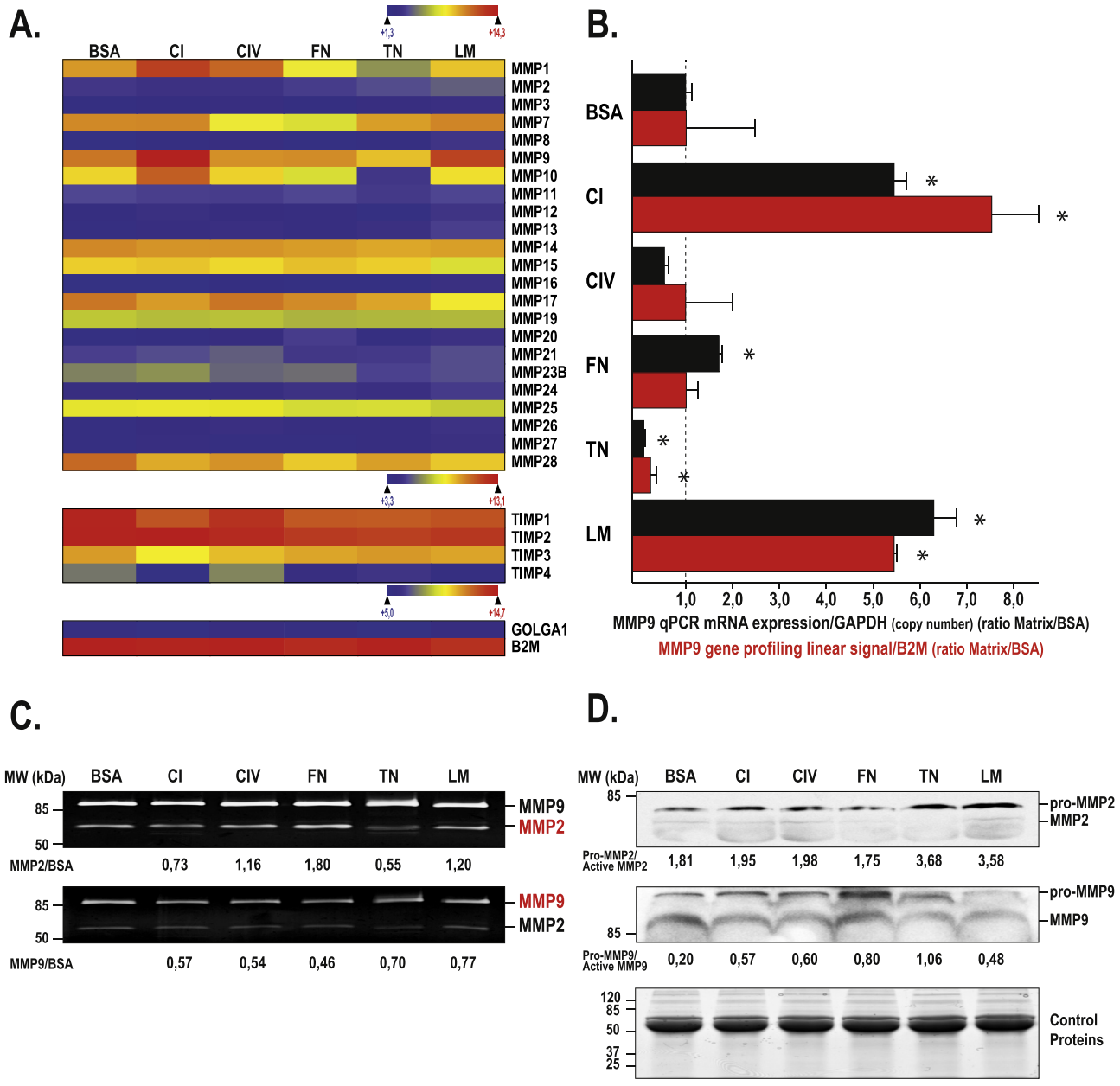

Fig. 6. Influence of individual ECM components on the expression of MMP genes. **A**: Heatmap representation of the expression profiles for all MMP and TIMP genes in HCECs grown on BSA or on individual ECM components (CI, CIV, FN, TN and LM). **B**: Comparison of MMP9 expression as measured by qPCR (black columns) and microarray (red columns). For qPCR analyses, data were expressed as the ratio of the MMP9 copy number (normalized to that of GAPDH) measured on the individual ECM components over that obtained on BSA. For microarray analyses, data were expressed as the ratio of the MMP9 linear signal (normalized to that of B2M) measured on the individual ECM components over that obtained on BSA. The statistical relevance of the data was analyzed by one-way ANOVA (Dunnett's post-test; $P < 0.05$). **C**: The enzymatic activity of both MMP2 and MMP9 was evaluated in the culture media of HCECs grown on BSA or on each of the individual ECM component by zymographic analyses. Both the MMP2 and MMP9 activity was quantified and expressed as the ratio of each MMP measured on each individual ECM component over that measured on BSA. The most relevant molecular mass markers (kDa) are also indicated on the left of each gel. **D**: Expression of both MMP2 and MMP9 was monitored by Western blot in total protein extracts prepared from HCECs grown on BSA and individual ECM components. Both the inactive (pro-) and active forms of the enzymes are indicated. The amount of MMP2 and MMP9 protein was quantified by densitometric analysis and expressed as the ratio of pro-MMP/active-MMP measured on each individual ECM component over that measured on BSA. Coomassie blue staining of proteins from each sample is also presented as a normalization control (bottom lane). (For interpretation of the references to colour in this figure legend, the reader is referred to the web version of this article.)

tissue [52]. However, we have shown a few years ago, that endothelial cells had no influence on the composition and organization of the BM in our model [20]. This apparent discrepancy can be explained, at least in part, by the differences between the 2 models: i) a combination of rabbit and mouse rather than human corneal cells were used and ii) rabbit corneal epithelial and stromal fibroblast cells were embedded into a collagen matrix rather than exploiting the matrix naturally secreted by the human stromal fibroblasts, as is the case in our reconstructed corneal tissues. Corneal models have also been produced with other cell types such as umbilical stem cells [53]. It would prove interesting to use these models to evaluate the impact of a different stroma on corneal healing.

Wound healing of the injured cornea would not be possible without significant alterations in the pattern of genes expressed by the epithelial cells bordering the damaged area. Although the most

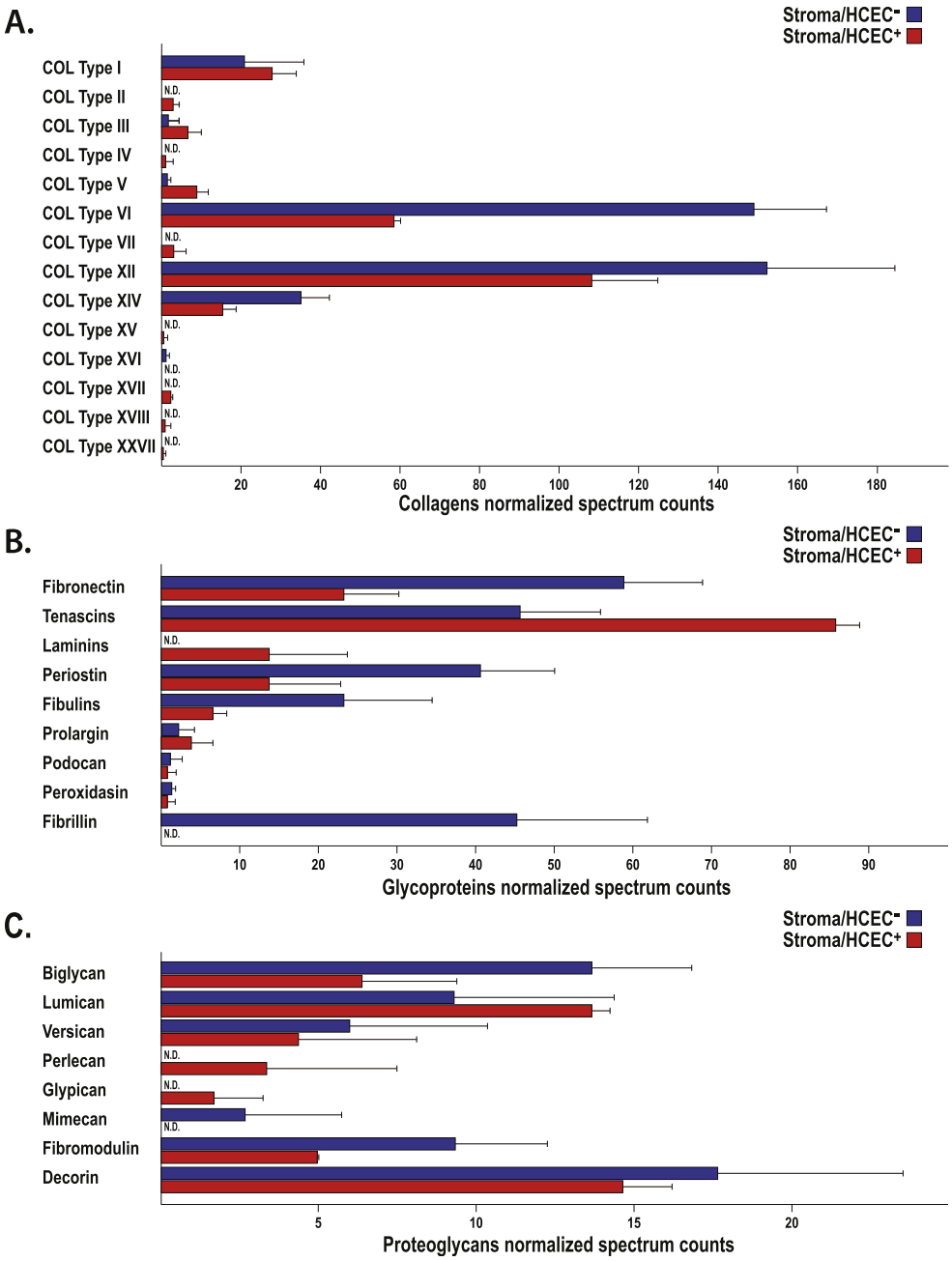

Fig. 7. Contribution of HCECs to the composition of the reconstructed corneal stroma. **A-C**: Mass spectrometry analysis of the ECM components from the reconstructed stromas alone (stroma/HCECs-) or seeded with HCECs and then raised to the air-liquid condition in order to produce a stratified corneal epithelium (stroma/HCECs+). Data are provided for the various types of collagens (panel **A**), glycoproteins (panel **B**) and proteoglycans (panel **C**) (n = 4). The value for each individual ECM component is expressed as the ratio of its normalized spectrum count.

dramatic change in the transcriptional pattern of deregulated genes occurs in the central wounded area (a total of 2754 genes), yet more than 2200 genes expressed by HCECs from the external ring have become deregulated by at least a 2-fold factor (1256 are commonly deregulated in both the central and external rings) despite that these cells were located far from the wounded area. Interestingly, of all these genes, 1098 were found to be deregulated in all three areas from the wounded corneas relative to their counterpart in the unwounded corneas (Fig. 2D), a clear indication that wound healing is still going on four days after wounding. These particularly interesting results suggest that the intact cells bordering the damaged area somehow transmit signals (diffusible or through cell-cell contacts) that move from cell to cell, like a wave effect, all over the intact section of the tissue-engineered cornea. In a recent study by Gao et al. [54], a similar signal wave was reported to occur upon scratch injury of primary cultured cerebral cortical astrocytes. This remarkable process was demonstrated to be caused by a calcium influx from the extracellular compartment, initially triggered by the scratch wound, that is then transmitted through gap junctions to the surrounding intact cells. One of the consequences of the sudden calcium influx is the activation of the JNK/c-Jun/AP-1 pathway. Interestingly, in the present study, transcription of the c-Jun subunit encoding gene was shown to be significantly increased in the central wound (average linear signal (ALS): 548.7)

Table 1
Average ECM peptide counts.

	Average ECM HCEC$^-$	Average ECM HCEC$^+$
COLLAGENS		
Collagen TYPE I	21.0 ± 15.1	28.0 ± 6.6
Collagen TYPE II	N.D.	3.0 ± 1.0
Collagen TYPE III	2.0 ± 2.6	6.7 ± 2.9
Collagen TYPE IV	N.D.	1.0 ± 1.7
Collagen TYPE V	1.7 ± 0.6	9.0 ± 3.0
Collagen TYPE VI	148.3 ± 18.8	59.0 ± 1.7
Collagen TYPE VII	N.D.	3.3 ± 3.1
Collagen TYPE XII	151.7 ± 32.3	108.3 ± 16.0
Collagen TYPE XIV	35.3 ± 7.5	15.7 ± 3.5
Collagen TYPE XV	N.D.	0.7 ± 1.2
Collagen TYPE XVI	1.3 ± 1.2	N.D.
Collagen TYPE XVII	N.D.	2.7 ± 0.6
Collagen TYPE XVIII	N.D.	1.0 ± 1.0
Collagen TYPE XXVII	N.D.	0.7 ± 1.2
Total Collagens	361.3	239.3
GLYCOPROTEINS		
Fibronectin	59.0 ± 9.6	23.3 ± 6.7
Tenascin	45.7 ± 10.3	85.7 ± 3.1
Laminin	N.D.	13.7 ± 9.9
Periostin	40.7 ± 9.5	13.7 ± 9.3
Fibulin	25.3 ± 11.1	6.7 ± 1.5
Prolargin	2.3 ± 2.1	4.0 ± 2.6
Podocan	1.0 ± 1.7	0.7 ± 1.2
Peroxidasin	1.3 ± 0.6	0.7 ± 1.2
Fibrillin	45.3 ± 16.4	N.D.
Total Glycoproteins	220.6	148.5
PROTEOGLYCANS		
Biglycan	13.7 ± 3.2	6.3 ± 3.1
Lumican	9.3 ± 5.0	13.7 ± 0.6
Versican	6.0 ± 4.4	4.3 ± 3.8
Perlecan	N.D.	3.3 ± 4.2
Glypican	N.D.	1.7 ± 1.5
Mimecan	2.7 ± 3.1	N.D.
Fibromodulin	9.3 ± 2.9	5.0 ± 2.9
Decorin	17.7 ± 5.9	14.7 ± 1.5
Total Proteoglycans	58.7	49.0
Total ECM peptides	640.6	436.6

and returned to the control level in the external ring (ALS: 208.9; Fig. 3 and Supplementary Table 2). Although scratch injury is well recognized as a model to study corneal wound healing, yet our study is the first to report the existence of such a signal wave and to examine its influence on global gene expression in a tissue-engineered, human corneal model. Alternatively, the differential gene regulatory effects we observed between the central and external areas of wounded corneas may also have resulted from cytokines and/or growth factors released in the culture media by the cells from the central wound. However, we believe this is highly improbable due to the fact that the reconstructed two-layers corneas were cultured at the air-liquid interface prior to wounding and that no culture medium was therefore present over the entire stratified corneal epithelium during wound closure, the reconstructed tissues being supplemented from their stromal compartment. Therefore, the 'signal wave' as detailed above remains a sounded possibility to explain our results.

The 55 most deregulated genes in the wounded corneas were organized into different classes (I, II and III) depending on how their expression evolves between the central, internal and external areas. Those from class I, such as VCAM1 and PAMR1, have their expression dramatically reduced in the central wound and remained low as we move away from the wounded area and never returned to their non-injured level. On the other hand, those that belong to what we defined as class II were strongly expressed in the central wound but tended to return to the level of the unwounded control as we moved away from the central area. Both MMP9 and MMP10 as well as the laminin α3 (LAMA3) and γ2 (LAMC2) genes belong to that category. Finally, those identified as class III genes suddenly became repressed in the central wound but as with the class II genes, they then tended to return to their normal control, unwounded level as we move away from the central area. No particular feature emerged from the analysis of the class I gene function. On the other hand, examination of the class II genes revealed that five of them (LAMA5, LAMC2, MMP9, MMP2 and MMP10) encode proteins that may contribute either to the composition or the remodeling of the ECM. In addition, three genes (LCE3D, SPRR2B and SPRR2D) encode proteins that are predominantly expressed in epithelial cells. Finally, two genes from class III (CDH2 and CRTAC1) encode proteins that participate to cell adhesion (also refer to Supplementary Table 2 for more details).

Gene profiling analysis conducted on our two-layers tissue-engineered corneas revealed often dramatic increases in the expression of the metalloproteinases-encoding genes MMP1, MMP2, MMP3, MMP9, MMP10, MMP11 and MMP13 in the central area of wounded, tissue-engineered corneal tissues, which is very similar to the pattern reported recently by Gordon et al. in a mouse corneal model of epithelial resurfacing [55]. MMP-9 is well known to be the primary MMP synthesized and secreted by basal corneal epithelial cells that migrate to cover the wound [56,57]. During rat corneal wound healing, expression of MMP1, MMP3, MMP7, MMP9 and MMP12 was also reported to increase in corneal epithelial cells [30]. Meanwhile, wound repair after keratectomy is also characterized by increased expression of MMP1, MMP2, MMP3 and MMP9 in the rabbit and rat corneas [31]. MMP13, along with MMP1 and MMP8, are collagenases capable of degrading native fibrillar collagens (type I, II, and III collagens). Lacking in normal control corneas, MMP13 mRNA has, however, been detected in the epithelial cells of wounded rat corneas [58] whereas MMP10 was shown to be overexpressed in the diabetic corneal epithelium [59]. In addition, expression of MMP3, MMP10 and MMP11, which could be detected in normal corneal epithelial cells, increases upon exposure to IL-1β and TNF-α [44]. The pattern of MMPs expressed in our healing, partial thickness tissue-engineered corneas is therefore consistent with the metalloproteinase activities observed in various corneal pathologies that require migration or replacement of the epithelial cells.

In our biomaterial model, the presence of stromal fibroblasts clearly impacted on the MMPs secreted by HCECs (in the stroma + condition) as they often triggered dramatic increases in the expression of MMP2, MMP3, MMP12, MMP13 and MMP24 that otherwise did not respond to the tissue-engineered ECM depleted of its fibroblasts (in the stroma-condition). It is also interesting to point out that the pattern of MMPs expressed by HCECs grown on the fibroblasts-containing stroma (Stroma+; Fig. 5A) is virtually identical to that seen in the central area of wounded partial thickness tissue-engineered corneas (Central; Fig. 3A) thereby suggesting that both the fibroblasts and the matrix they secrete are required to allow the expression of the appropriate combination of MMPs during corneal wound healing. This result clearly suggests that stromal fibroblasts do produce diffusible factors that then trigger HCECs to increase the transcription of these MMP genes as well as that of other genes whose encoded products are required for wound healing, such as integrins and ECM component encoding genes [51]. Indeed, MMPs expression in the cornea has been shown to be modulated by cytokines (such as IL-1β and IL-6 [60,61]) and growth factors (such as TGFβ [62,63]) through alteration in the expression and/or properties of a few transcription factors such as AP-1 [61] and Sp1 [64]. The requirement for soluble factors secreted by living stromal fibroblasts is in agreement with our previous observation that corneal fibroblasts contribute to the differentiation and stratification properties of HCECs [14]. Consistent with the above studies, we also identified IL-6 as one such soluble factor

[14]. Transcription of the IL-6 encoding gene was also found to increase considerably in the central wound of our partial thickness tissue-engineered corneas relative to both the internal and external rings (ALS: 576.8, 165.0 and 184.0 for central, internal and external areas, respectively). Interestingly, expression of MMP1, MMP3, MMP10, MMP11 and MMP13 has been reported to be dose dependently upregulated by IL-1β and TNF-α in corneal epithelial cells [44], which is also consistent with the dramatic increase in the expression of IL-1β (ALS: 316.2, 50.8 and 10.7 for central, internal and external areas, respectively) and TNF-α (ALS: 69.3, 13.9 and 16.4 for central, internal and external areas, respectively) we observed in the central area of wounded tissue-engineered corneas (Fig. 3C and Supplementary Table 2). Meanwhile, Kim et al. demonstrated clearly that TGF-β1 exerts a positive regulatory influence on the expression and production of gelatinase (MMP9), collagenases (MMP1, MMP13) and stromelysins (MMP3, MMP10, MMP11) in HCECs cultured in monolayers and suggested that TGF-β1 may play a role in the pathogenesis of MMP mediated ocular surface diseases, such as sterile corneal ulceration [63]. This may explain at least in part the dramatic increase in the expression of MMP1, MMP2, MMP3, MMP9, MMP10, MMP11 and MMP13 that we observed in the wounded tissues of our two-layers tissue-engineered corneas as increases in the expression of both TGF-β1 (ALS: 312.6, 212.1 and 171.8 for central, internal and external areas, respectively) and TGF-β3 (ALS: 537.6, 90.3 and 68.2 for central, internal and external areas, respectively) were also observed in the central wounds relative to the controls (Fig. 3C and Supplementary Table 2).

One particularly unique aspect of our study is the demonstration that HCECs are required, together with stromal fibroblasts, to secrete and organize an ECM that is very close to that seen in the native cornea. This may depend in part from the inability of stromal fibroblasts to organize a typical BM without interactions with epithelial cells. The epithelial cells from the two-layers tissue-engineered human cornea were demonstrated to secrete and organize such a typical BM [15–17] although its precise composition had never been precisely determined before. In the native cornea, the BM on which epithelial cells attach is enriched in various types of collagens (IV, VII, XII, XVII, XVIII), laminins (LM-111, LM-332, LM-311, LM-411, LM-511), nidogen, perlecan and small amounts of FN [65–72]. With the exception of CXII and FN, none of these BM components could be detected in the tissue-engineered stroma that has not been added HCECs (stroma/HCEC$^-$). On the other hand, they all could be detected, although at low levels, when a corneal epithelial layer was present (stroma/HCEC$^+$), a clear indication that organization of the corneal BM do require the presence of a corneal epithelial layer. The very low level of CIV in the stroma/HCEC$^+$ tissue-engineered corneas, which is normally present in the corneal BM and the Descemet's membrane but absent from the corneal stroma [73], may be accounted for by the lack of maturity of the BM beneath the stratified epithelium as a result of a rather short culture period (7 days) at the air-liquid interface. Reduced levels of CIV (as well as that of other collagen types) may also have resulted from the fact that it is a substrate of many MMPs, including MMP9 and MMP10, whose expression is dramatically increased during wound healing. Unlike for the BM components, all those from the corneal stroma, which comprise collagen types I, III, V, VI, XII, XIV, and various proteoglycans (decorin, lumican and mimecan) can be observed in the stroma of our tissue-engineered corneas in the absence of an epithelial layer (stroma/HCEC$^-$) [68,74–76]. These results are also consistent with those reported in a recent study by Gendron and Rochette [77] who used tissue-engineered human corneal stromas in order to examine the change in the ECM composition upon exposure of the tissue-engineered stromas to UV light. Finally, the Bowman's membrane has been shown to contain collagen types I, III, IV, V, VI, VII and XII (of which both CIV and CVII were thought to come from the corneal BM) [69,78–80], all of which could be detected in the matrix from the tissue-engineered corneas grown with an epithelial layer (stroma/HCEC$^+$).

Our results suggest that expression of LM, glypican and perlecan in the stromal and basal ECM matrix is dependent on the presence of HCECs. Laminins are normal constituents of the corneal BM and have been shown to be secreted by the basal cells (primarily LM-5) from the corneal epithelium and also suggested to be produced (for LM-10) by stromal fibroblasts [81]. Deregulated expression of glypican has been shown to be associated with wound healing of the mouse cornea [82]. Interestingly, perlecan, an heparin sulfate proteoglycan that cross-links many components from the ECM and cell surface molecules, is a constituent of the normal, unwounded corneal BM [70].

When tested individually, some of the ECM components clearly altered the pattern of MMP genes expressed by HCECs when grown as a monolayer. This was particularly noticeable for both MMP1 and MMP9. Indeed, whereas CI influenced positively the expression of both MMP1 and MMP9, TN, on the other hand, severely repressed their transcription (as well as that of MMP10). In addition, LM also increased expression of MMP9, which is consistent with the observation that silencing expression of LM alpha-4 chain also decreased MMP9 expression in extravillous explants and HTR8/SVneo cells [83]. Furthermore, cells from human oral squamous cell carcinoma (OSCC), adenoid cystic carcinoma (CAC2) and myoepithelioma (M1) exposed to the LM alpha1 chain peptide AG73 also had increased MMP9 activity [84,85]. Therefore, LM has obviously a positive influence on the expression of the MMP9 gene. However, the true significance of these alterations in the expression of MMPs by individual ECM components at the transcriptional level remains elusive as no corresponding changes were observed in the expression and enzymatic activity of these enzymes at the protein level.

5. Conclusion

In this study, we demonstrated that the two-layers tissue-engineered human cornea used as a biomaterial substitute is an outstanding model to study the expression of MMP genes, as well as that of other genes, that play pivotal functions in the remodeling of the ECM during corneal wound healing. Altering expression of these ECM remodeling enzymes in the tissue-engineered cornea with the aim of improving the dynamic of wound closure should prove a safe and practical procedure and a prerequisite to the use of animal models.

Acknowledgments

This study was supported by a grant from the 'Canadian Institutes of Health Research' (CIHR) (MOP-53170) to L.G., S.L.G and François A. Auger. The Banque d'yeux Nationale is partly supported by the Réseau de Recherche en Santé de la Vision from the 'Fonds de Recherche du Québec-Santé' (FRQS). C.C. was supported by a studentship from the FRQS. L.G. is the recipient of a Tier 1 Canadian Research Chair on Stem Cell and Tissue Engineering.

Appendix A. Supplementary data

Supplementary data related to this article can be found at http://dx.doi.org/10.1016/j.biomaterials.2015.11.006.

References

[1] V.B. Agrawal, R.J. Tsai, Corneal epithelial wound healing, Indian J. Ophthalmol.

51 (2003) 5–15.
[2] L. Taliana, M.D. Evans, S.D. Dimitrijevich, J.G. Steele, Vitronectin or fibronectin is required for corneal fibroblast-seeded collagen gel contraction, Invest Ophthalmol. Vis. Sci. 41 (2000) 103–109.
[3] J.P. Whitcher, M. Srinivasan, M.P. Upadhyay, Corneal blindness: a global perspective, Bull. World Health Organ. 79 (2001) 214–221.
[4] F.A. Woreta, G.W. Davis, K.S. Bower, LASIK and surface ablation in corneal dystrophies, Surv. Ophthalmol. 60 (2015) 115–122.
[5] R.K. Brazzell, M.E. Stern, J.V. Aquavella, R.W. Beuerman, L. Baird, Human recombinant epidermal growth factor in experimental corneal wound healing, Invest. Ophthalmol. Vis. Sci. 32 (1991) 336–340.
[6] K. Burling, M.A. Seguin, P. Marsh, K. Brinkman, J. Madigan, M. Thurmond, et al., Effect of topical administration of epidermal growth factor on healing of corneal epithelial defects in horses, Am. J. Vet. Res. 61 (2000) 1150–1155.
[7] M.B. Grant, P.T. Khaw, G.S. Schultz, J.L. Adams, R.W. Shimizu, Effects of epidermal growth factor, fibroblast growth factor, and transforming growth factor-beta on corneal cell chemotaxis, Invest. Ophthalmol. Vis. Sci. 33 (1992) 3292–3301.
[8] M.J. Kim, R.M. Jun, W.K. Kim, H.J. Hann, Y.H. Chong, H.Y. Park, et al., Optimal concentration of human epidermal growth factor (hEGF) for epithelial healing in experimental corneal alkali wounds, Curr. Eye Res. 22 (2001) 272–279.
[9] B.A. Maldonado, L.T. Furcht, Epidermal growth factor stimulates integrin-mediated cell migration of cultured human corneal epithelial cells on fibronectin and arginine-glycine-aspartic acid peptide, Invest. Ophthalmol. Vis. Sci. 36 (1995) 2120–2126.
[10] J.D. Nelson, V. Silverman, P.H. Lima, G. Beckman, Corneal epithelial wound healing: a tissue culture assay on the effect of antibiotics, Curr. Eye Res. 9 (1990) 277–285.
[11] S.J. Simmons, M.M. Jumblatt, A.H. Neufeld, Corneal epithelial wound closure in tissue culture: an in vitro model of ocular irritancy, Toxicol. Appl. Pharmacol. 88 (1987) 13–23.
[12] J.D. Zieske, A.E. Hutcheon, X. Guo, E.H. Chung, N.C. Joyce, TGF-beta receptor types I and II are differentially expressed during corneal epithelial wound repair, Invest. Ophthalmol. Vis. Sci. 42 (2001) 1465–1471.
[13] C.E. Ghezzi, J. Rnjak-Kovacina, D.L. Kaplan, Corneal tissue engineering: recent advances and future perspectives, Tissue Eng. Part B Rev. 21 (2015) 276–287.
[14] P. Carrier, A. Deschambeault, C. Audet, M. Talbot, R. Gauvin, C.J. Giasson, et al., Impact of cell source on human cornea reconstructed by tissue engineering, Invest. Ophthalmol. Vis. Sci. 50 (2009) 2645–2652.
[15] P. Carrier, A. Deschambeault, M. Talbot, C.J. Giasson, F.A. Auger, S.L. Guerin, et al., Characterization of wound reepithelialization using a new human tissue-engineered corneal wound healing model, Invest. Ophthalmol. Vis. Sci. 49 (2008) 1376–1385.
[16] L. Germain, F.A. Auger, E. Grandbois, R. Guignard, M. Giasson, H. Boisjoly, et al., Reconstructed human cornea produced in vitro by tissue engineering, Pathobiology 67 (1999) 140–147.
[17] L. Germain, P. Carrier, F.A. Auger, C. Salesse, S.L. Guerin, Can we produce a human corneal equivalent by tissue engineering? Prog. Retin Eye Res. 19 (2000) 497–527.
[18] L. Germain, C. Giasson, P. Carrier, S.L. Guérin, C. Salesse, F.A. Auger, Tissue Engineering of Human Cornea, in: G.E. Wnek, G.L. Bowling (Eds.), Encyclopedia of Biomaterials and Biomedical Engineering, Marcel Dekker, New York, 2004, pp. 1534–1544.
[19] C. Paquet, D. Larouche, F. Bisson, S. Proulx, C. Simard-Bisson, M. Gaudreault, et al., Tissue engineering of skin and cornea: Development of new models for in vitro studies, Ann. N. Y. Acad. Sci. 1197 (2010) 166–177.
[20] S. Proulx, J. d'Arc Uwamaliya, P. Carrier, A. Deschambeault, C. Audet, C.J. Giasson, et al., Reconstruction of a human cornea by the self-assembly approach of tissue engineering using the three native cell types, Mol. Vis. 16 (2010) 2192–2201.
[21] M. Michel, N. L'Heureux, R. Pouliot, W. Xu, F.A. Auger, L. Germain, Characterization of a new tissue-engineered human skin equivalent with hair, Vitro Cell. Dev. Biol. Anim. 35 (1999) 318–326.
[22] R. Pouliot, D. Larouche, F.A. Auger, J. Juhasz, W. Xu, H. Li, et al., Reconstructed human skin produced in vitro and grafted on athymic mice, Transplantation 73 (2002) 1751–1757.
[23] C. Gaal, German physicians–decimated by ageing, low spirit, and changing attitude to life, Orv. Hetil. 143 (2002) 2449–2451.
[24] L.A. Liotta, E.C. Kohn, The microenvironment of the tumour-host interface, Nature 411 (2001) 375–379.
[25] C. Streuli, Extracellular matrix remodelling and cellular differentiation, Curr. Opin. cell Biol. 11 (1999) 634–640.
[26] S. Filippov, G.C. Koenig, T.H. Chun, K.B. Hotary, I. Ota, T.H. Bugge, et al., MT1-matrix metalloproteinase directs arterial wall invasion and neointima formation by vascular smooth muscle cells, J. Exp. Med. 202 (2005) 663–671.
[27] K. Holmbeck, P. Bianco, J. Caterina, S. Yamada, M. Kromer, S.A. Kuznetsov, et al., MT1-MMP-deficient mice develop dwarfism, osteopenia, arthritis, and connective tissue disease due to inadequate collagen turnover, Cell. 99 (1999) 81–92.
[28] S.D. Shapiro, Matrix metalloproteinase degradation of extracellular matrix: biological consequences, Curr. Opin. cell Biol. 10 (1998) 602–608.
[29] J.M. Sivak, M.E. Fini, MMPs in the eye: emerging roles for matrix metalloproteinases in ocular physiology, Prog. Retin. Eye Res. 21 (2002) 1–14.
[30] J. Lyu, C.K. Joo, Wnt-7a up-regulates matrix metalloproteinase-12 expression and promotes cell proliferation in corneal epithelial cells during wound healing, J. Biol. Chem. 280 (2005) 21653–21660.
[31] B. Mulholland, S.J. Tuft, P.T. Khaw, Matrix metalloproteinase distribution during early corneal wound healing, Eye (Lond) 19 (2005) 584–588.
[32] S. Chakraborti, M. Mandal, S. Das, A. Mandal, T. Chakraborti, Regulation of matrix metalloproteinases: an overview, Mol. Cell Biochem. 253 (2003) 269–285.
[33] G.M. Gordon, D.R. Ledee, W.J. Feuer, M.E. Fini, Cytokines and signaling pathways regulating matrix metalloproteinase-9 (MMP-9) expression in corneal epithelial cells, J. Cell Physiol. 221 (2009) 402–411.
[34] C.K. Joo, Y. Seomun, Matrix metalloproteinase (MMP) and TGF beta 1-stimulated cell migration in skin and cornea wound healing, Cell Adh. Migr. 2 (2008) 252–253.
[35] M. Jovanovic, I. Stefanoska, L. Radojcic, L. Vicovac, Interleukin-8 (CXCL8) stimulates trophoblast cell migration and invasion by increasing levels of matrix metalloproteinase (MMP)2 and MMP9 and integrins alpha5 and beta1, Reproduction 139 (2010) 789–798.
[36] M. Gaudreault, P. Carrier, K. Larouche, S. Leclerc, M. Giasson, L. Germain, et al., Influence of sp1/sp3 expression on corneal epithelial cells proliferation and differentiation properties in reconstructed tissues, Invest. Ophthalmol. Vis. Sci. 44 (2003) 1447–1457.
[37] M. Gaudreault, F. Vigneault, S. Leclerc, S.L. Guerin, Laminin reduces expression of the human alpha6 integrin subunit gene by altering the level of the transcription factors Sp1 and Sp3, Invest. Ophthalmol. Vis. Sci. 48 (2007) 3490–3505.
[38] K. Larouche, S. Leclerc, C. Salesse, S.L. Guerin, Expression of the alpha 5 integrin subunit gene promoter is positively regulated by the extracellular matrix component fibronectin through the transcription factor Sp1 in corneal epithelial cells in vitro, J. Biol. Chem. 275 (2000) 39182–39192.
[39] C. Duval, K. Zaniolo, S. Leclerc, C. Salesse, S.L. Guerin, Characterization of the human alpha9 integrin subunit gene: Promoter analysis and transcriptional regulation in ocular cells, Exp. Eye Res. 135 (2015) 146–163.
[40] A. Keller, A.I. Nesvizhskii, E. Kolker, R. Aebersold, Empirical statistical model to estimate the accuracy of peptide identifications made by MS/MS and database search, Anal. Chem. 74 (2002) 5383–5392.
[41] A.I. Nesvizhskii, A. Keller, E. Kolker, R. Aebersold, A statistical model for identifying proteins by tandem mass spectrometry, Anal. Chem. 75 (2003) 4646–4658.
[42] M.E. Gingras, K. Larouche, N. Larouche, S. Leclerc, C. Salesse, S.L. Guerin, Regulation of the integrin subunit alpha5 gene promoter by the transcription factors Sp1/Sp3 is influenced by the cell density in rabbit corneal epithelial cells, Invest. Ophthalmol. Vis. Sci. 44 (2003) 3742–3755.
[43] A. Beliveau, M. Berube, A. Rousseau, G. Pelletier, S.L. Guerin, Expression of integrin alpha5beta1 and MMPs associated with epithelioid morphology and malignancy of uveal melanoma, Invest. Ophthalmol. Vis. Sci. 41 (2000) 2363–2372.
[44] D.Q. Li, T.Y. Shang, H.S. Kim, A. Solomon, B.L. Lokeshwar, S.C. Pflugfelder, Regulated expression of collagenases MMP-1, -8, and -13 and stromelysins MMP-3, -10, and -11 by human corneal epithelial cells, Invest. Ophthalmol. Vis. Sci. 44 (2003) 2928–2936.
[45] J. Imanishi, K. Kamiyama, I. Iguchi, M. Kita, C. Sotozono, S. Kinoshita, Growth factors: importance in wound healing and maintenance of transparency of the cornea, Prog. Retin. Eye Res. 19 (2000) 113–129.
[46] S. O'Kane, M.W. Ferguson, Transforming growth factor beta s and wound healing, Int. J. Biochem. cell Biol. 29 (1997) 63–78.
[47] K. Philipp, F. Riedel, M. Sauerbier, K. Hormann, G. Germann, Targeting TGF-beta in human keratinocytes and its potential role in wound healing, Int. J. Mol. Med. 14 (2004) 589–593.
[48] S. Saika, TGF-beta signal transduction in corneal wound healing as a therapeutic target, Cornea 23 (2004) S25–S30.
[49] M.M. Santoro, G. Gaudino, Cellular and molecular facets of keratinocyte reepithelization during wound healing, Exp. Cell Res. 304 (2005) 274–286.
[50] L. Lu, P.S. Reinach, W.W. Kao, Corneal epithelial wound healing, Exp. Biol. Med. (Maywood) 226 (2001) 653–664.
[51] J. Lake, K. Zaniolo, M. Gaudreault, P. Carrier, A. Deschambault, R. Bazin, et al., Expression of the alpha5 integrin gene in corneal epithelial cells cultured on tissue-engineered human extracellular matrices, Biomaterials 34 (2013) 6367–6376.
[52] J.D. Zieske, V.S. Mason, M.E. Wasson, S.F. Meunier, C.J. Nolte, N. Fukai, et al., Basement membrane assembly and differentiation of cultured corneal cells: importance of culture environment and endothelial cell interaction, Exp. Cell Res. 214 (1994) 621–633.
[53] I. Garzon, M.A. Martin-Piedra, C. Alfonso-Rodriguez, M. Gonzalez-Andrades, V. Carriel, C. Martinez-Gomez, et al., Generation of a biomimetic human artificial cornea model using Wharton's jelly mesenchymal stem cells, Invest. Ophthalmol. Vis. Sci. 55 (2014) 4073–4083.
[54] K. Gao, C.R. Wang, F. Jiang, A.Y. Wong, N. Su, J.H. Jiang, et al., Traumatic scratch injury in astrocytes triggers calcium influx to activate the JNK/c-Jun/AP-1 pathway and switch on GFAP expression, Glia 61 (2013) 2063–2077.
[55] G.M. Gordon, J.S. Austin, A.L. Sklar, W.J. Feuer, A.J. LaGier, M.E. Fini, Comprehensive gene expression profiling and functional analysis of matrix metalloproteinases and TIMPs, and identification of ADAM-10 gene expression, in a corneal model of epithelial resurfacing, J. Cell Physiol. 226 (2011) 1461–1470.
[56] M.E. Fini, M.T. Girard, M. Matsubara, J.D. Bartlett, Unique regulation of the matrix metalloproteinase, gelatinase B, Invest. Ophthalmol. Vis. Sci. 36 (1995) 622–633.

[57] M. Matsubara, M.T. Girard, C.L. Kublin, C. Cintron, M.E. Fini, Differential roles for two gelatinolytic enzymes of the matrix metalloproteinase family in the remodelling cornea, Dev. Biol. 147 (1991) 425–439.
[58] H.Q. Ye, M. Maeda, F.S. Yu, D.T. Azar, Differential expression of MT1-MMP (MMP-14) and collagenase III (MMP-13) genes in normal and wounded rat corneas, Invest. Ophthalmol. Vis. Sci. 41 (2000) 2894–2899.
[59] M. Saghizadeh, D.J. Brown, R. Castellon, M. Chwa, G.H. Huang, J.Y. Ljubimova, et al., Overexpression of matrix metalloproteinase-10 and matrix metalloproteinase-3 in human diabetic corneas: a possible mechanism of basement membrane and integrin alterations, Am. J. pathol. 158 (2001) 723–734.
[60] J.A. Ko, T. Chikama, K.H. Sonoda, Y. Kiuchi, Up-regulation of matrix metalloproteinase-1 and interleukin-6 expression in cocultures of corneal fibroblasts and neural cells, Biochem. Biophys. Res. Commun. 419 (2012) 537–542.
[61] H.C. Tseng, I.T. Lee, C.C. Lin, P.L. Chi, S.E. Cheng, R.H. Shih, et al., IL-1beta promotes corneal epithelial cell migration by increasing MMP-9 expression through NF-kappaB- and AP-1-dependent pathways, PloS one 8 (2013) e57955.
[62] M.T. Girard, M. Matsubara, M.E. Fini, Transforming growth factor-beta and interleukin-1 modulate metalloproteinase expression by corneal stromal cells, Invest. Ophthalmol. Vis. Sci. 32 (1991) 2441–2454.
[63] H.S. Kim, T. Shang, Z. Chen, S.C. Pflugfelder, D.Q. Li, TGF-beta1 stimulates production of gelatinase (MMP-9), collagenases (MMP-1, -13) and stromelysins (MMP-3, -10, -11) by human corneal epithelial cells, Exp. Eye Res. 79 (2004) 263–274.
[64] V.S. Reddy, S.D. Prabhu, S. Mummidi, A.J. Valente, B. Venkatesan, P. Shanmugam, et al., Interleukin-18 induces EMMPRIN expression in primary cardiomyocytes via JNK/Sp1 signaling and MMP-9 in part via EMMPRIN and through AP-1 and NF-kappaB activation, Am. J. Physiol. Heart Circ. Physiol. 299 (2010) H1242–H1254.
[65] A. Kabosova, D.T. Azar, G.A. Bannikov, K.P. Campbell, M. Durbeej, R.F. Ghohestani, et al., Compositional differences between infant and adult human corneal basement membranes, Invest. Ophthalmol. Vis. Sci. 48 (2007) 4989–4999.
[66] A.V. Ljubimov, R.E. Burgeson, R.J. Butkowski, A.F. Michael, T.T. Sun, M.C. Kenney, Human corneal basement membrane heterogeneity: topographical differences in the expression of type IV collagen and laminin isoforms, Lab. Invest.; A J. Tech. Methods Pathol. 72 (1995) 461–473.
[67] G.R. Martin, R. Timpl, Laminin and other basement membrane components, Annu. Rev. cell Biol. 3 (1987) 57–85.
[68] Y.M. Michelacci, Collagens and proteoglycans of the corneal extracellular matrix, Braz. J. Med. Biol. Res. Revista brasileira de pesquisas medicas e biologicas/Sociedade Brasileira de Biofisica [et al] 36 (2003) 1037–1046.
[69] K. Nakayasu, M. Tanaka, H. Konomi, T. Hayashi, Distribution of types I, II, III, IV and V collagen in normal and keratoconus corneas, Ophthalmic Res. 18 (1986) 1–10.
[70] A.A. Torricelli, G.K. Marino, A. Santhanam, J. Wu, A. Singh, S.E. Wilson, Epithelial basement membrane proteins perlecan and nidogen-2 are up-regulated in stromal cells after epithelial injury in human corneas, Exp. Eye Res. 134 (2015) 33–38.
[71] A.A. Torricelli, V. Singh, M.R. Santhiago, S.E. Wilson, The corneal epithelial basement membrane: structure, function, and disease, Invest. Ophthalmol. Vis. Sci. 54 (2013) 6390–6400.
[72] A. Tuori, H. Uusitalo, R.E. Burgeson, J. Terttunen, I. Virtanen, The immunohistochemical composition of the human corneal basement membrane, Cornea 15 (1996) 286–294.
[73] U. Schlotzer-Schrehardt, B.O. Bachmann, T. Tourtas, A.A. Torricelli, A. Singh, S. Gonzalez, et al., Ultrastructure of the posterior corneal stroma, Ophthalmology 122 (2015) 693–699.
[74] K.M. Meek, N.J. Fullwood, Corneal and scleral collagens–a microscopist's perspective, Micron 32 (2001) 261–272.
[75] D.A. Newsome, J. Gross, J.R. Hassell, Human corneal stroma contains three distinct collagens, Invest. Ophthalmol. Vis. Sci. 22 (1982) 376–381.
[76] L. Robert, J.M. Legeais, A.M. Robert, G. Renard, Corneal collagens, Pathol. Biol. 49 (2001) 353–363.
[77] S.P. Gendron, P.J. Rochette, Modifications in stromal extracellular matrix of aged corneas can be induced by ultraviolet A irradiation, Aging cell 14 (2015) 433–442.
[78] I.E. Jacobsen, O.A. Jensen, J.U. Prause, Structure and composition of Bowman's membrane. Study by frozen resin cracking, Acta Ophthalmol. 62 (1984) 39–53.
[79] G.E. Marshall, A.G. Konstas, W.R. Lee, Immunogold fine structural localization of extracellular matrix components in aged human cornea. II. Collagen types V and VI, Graefe's Arch. for Clin. and Exp. Ophthalmol. Albrecht von Graefes Archiv fur klinische und experimentelle Ophthalmologie 229 (1991) 164–171.
[80] G.E. Marshall, A.G. Konstas, W.R. Lee, Immunogold fine structural localization of extracellular matrix components in aged human cornea. I. Types I-IV collagen and laminin, Graefe's Arch. for Clin. and Exp. Ophthalmol. Albrecht von Graefes Archiv fur klinische und experimentelle Ophthalmologie 229 (1991) 157–163.
[81] S. Filenius, M. Hormia, J. Rissanen, R.E. Burgeson, Y. Yamada, K. Araki-Sasaki, et al., Laminin synthesis and the adhesion characteristics of immortalized human corneal epithelial cells to laminin isoforms, Exp. Eye Res. 72 (2001) 93–103.
[82] C. Saravanan, Z. Cao, S.R. Head, N. Panjwani, Analysis of differential expression of glycosyltransferases in healing corneas by glycogene microarrays, Glycobiology 20 (2010) 13–23.
[83] N. Shan, X. Zhang, X. Xiao, H. Zhang, C. Tong, X. Luo, et al., Laminin alpha4 (LAMA4) expression promotes trophoblast cell invasion, migration, and angiogenesis, and is lowered in preeclamptic placentas, Placenta 36 (2015) 809–820.
[84] A.S. Siqueira, L.N. Gama-de-Souza, M.V. Arnaud, J.J. Pinheiro, R.G. Jaeger, Laminin-derived peptide AG73 regulates migration, invasion, and protease activity of human oral squamous cell carcinoma cells through syndecan-1 and beta1 integrin, Tumour Biol. the J. Int. Soc. for Oncodev. Biol. and Med. 31 (2010) 46–58.
[85] L.N. Gama-de-Souza, E. Cyreno-Oliveira, V.M. Freitas, E.S. Melo, V.F. Vilas-Boas, A.S. Moriscot, et al., Adhesion and protease activity in cell lines from human salivary gland tumors are regulated by the laminin-derived peptide AG73, syndecan-1 and beta1 integrin, Matrix Biol. J. Int. Soc. for Matrix Biol. 27 (2008) 402–419.